ATOMINSTITUT

Diese Dissertation haben begutachtet:

12.10.2015

DISSERTATION

Quantification and Production of Radioxenon Isotopes

for Nuclear Explosion Monitoring

ausgeführt zum Zwecke der Erlangung des akademischen Grades eines

Doktors der technischen Wissenschaften unter der Leitung von

Ao. Univ. Prof. i. R. Dipl.-Ing. Dr. techn. Helmuth Böck

eingereicht am Atominstitut der technischen Universität Wien von

Mag. rer. nat. Michael Lechermann

Matrikelnummer: 0135101

Pantzergasse 2/34

A-1190 Wien

Wien, am 1. Oktober 2015

933.090 II

Abstract

The Comprehensive Nuclear-Test-Ban Treaty (CTBT) forbids its state signatories all types of nuclear weapons tests. In support of the verification of compliance with the treaty the International Monitoring System (IMS), a worldwide network of seismic, hydro-acoustic, infrasound and radionuclide sensors, is currently being established.

Measurement of atmospheric radioxenon plays a key role in the identification of clandestine nuclear weapons tests, since it can provide unambiguous proof of the nuclear nature of suspicious events. A total of 40 radioxenon sampling stations continuously sample and analyze atmospheric radioxenon and transmit results to the International Data Centre (IDC) in Vienna, Austria.

The Austrian laboratory ATL03 is one of the 16 designated laboratories within the IMS that have the task to support the radionuclide stations as part of the quality assurance program. Therefore, a radioxenon laboratory measurement system has been developed, the Austrian Xenon Laboratory (AXeL).

AXeL can process and analyze atmospheric gas samples according to their stable xenon content and radioxenon activities of the four CTBT-relevant radioxenon isotopes ^{131m}Xe, ^{133m}Xe, ^{133}Xe and ^{135}Xe. The performance of the AXeL system has been tested and validated thoroughly in experiments and international intercomparison exercises. In December 2014 the ATL03 has been certified by the CTBTO as the first noble gas laboratory within the IMS.

Testing and validation is necessarily linked to the availability and application of radioxenon isotopes. Therefore, methods of radioxenon isotope production have been developed at ATL03. The two Austrian Xenon Generators AXG1 and AXG2 take advantage of the spontaneous fission decay branch of ^{252}Cf respectively the radioactive decay of ^{131}I to produce the four CTBT-relevant radioxenon isotopes in suitable activities.

KURZFASSUNG

Der umfassende Kernwaffenteststopp-Vertrag (CTBT) untersagt seinen Unterzeichnerstaaten jede Art von Kernwaffentest und die Beihilfe dazu. Um die Einhaltung des Vertrages sicherzustellen wird momentan ein weltweites internationales Überwachungssystem (IMS) errichtet. Es besteht aus seismischen und hydro-akustischen sowie für Infraschall und Radionuklide empfindlichen Sensoren.

Die Messung von atmosphärischem Radioxenon spielt hierbei eine Schlüsselrolle in der Auffindung von verdeckt durchgeführten Kernwaffentests, denn sie ermöglicht es, eindeutige Beweise zum nuklearen Charakter eines als verdächtig eingestuften Ereignisses zu erbringen. Insgesamt 40 Probennahmestationen für Radioxenon saugen ohne Unterbrechung atmosphärische Luft an, analysieren diese und senden die Ergebnisse an das Internationale Datenzentrum (IDC) in Wien.

Das österreichische Labor ATL03 ist eines der 16 vorgesehenen Labors des IMS, die die Aufgabe haben, die Radionuklidstationen als Teil des Programms zur Qualitätssicherung zu unterstützen. Aus diesem Grund wurde ein Radioxenon Laborsystem entwickelt, das Austrian Xenon Laboratory (AXeL).

AXeL kann atmosphärische Gasproben aufbereiten und auf ihren Anteil an stabilem Xenon und den Aktivitäten der vier CTBT-relevanten Radioxenonisotope ^{131m}Xe, ^{133m}Xe, ^{133}Xe and ^{135}Xe hin untersuchen. AXeL wurde in Experimenten ausgiebig getestet und in internationalen Ringversuchen validiert. Im Dezember 2014 wurde das ATL03 von der CTBTO als weltweit erstes Edelgaslabor des IMS für die Messung von Radioxenon zertifiziert.

Tests und Validierungen sind untrennbar mit der Verfügbarkeit und der Anwendung von Radioxenonisotopen verbunden. Deshalb wurden Methoden zur Produktion von Radioxenonisotopen vor Ort entwickelt. Die beiden Austrian Xenon Generators AXG1 und AXG2 basieren auf der Eigenschaft von ^{252}Cf zur Spontanspaltung beziehungsweise den radioaktiven Zerfall von ^{131}I um die vier Radioxenonisotope in ausreichenden Aktivitäten herzustellen.

Contents

List of Tables

List of Figures

Acronyms and Abbreviations

1 Introduction

1.1 Nuclear weapons tests

The devastating effects of nuclear weapons became manifest to the world by the end of the Second World War. The droppings of the nuclear bombs on Hiroshima and Nagasaki have killed at least 103,000 people within four months after the attacks. Long term effects are believed to have caused even more deaths (Oughterson and Shields, 1956). To this day, the cities' names stand for massive destruction and immeasurable suffering. The immense power of such weapons quickly gave them an infamous role in global politics. During the cold war, a nuclear arms race unfolded between the United States of America and the former Soviet Union and their respective allies. While both sides competed for supremacy in nuclear warfare, the nuclear stockpiles grew and with them nuclear testing.

Nuclear weapons tests in general serve the purpose of enhancing weapons characteristics, since they allow detailed insight into the physics of nuclear explosions. Testing of a device gives valuable information on its basic parameters of the design, most importantly the yield. Early developments quickly lead to more complex and powerful weapon designs like fusion-boosted fission weapons or the Teller-Ulam design, a multi-stage design for thermonuclear bombs. Nuclear testing has also been used to study the effects of nuclear explosions and radiation on organisms and structures. Starting with the Trinity test in 1945, by 2014 the world has seen a total of 2053 nuclear weapons tests (NRDC, 2006, 2007; NRDC Archive, 2007; Mikhailov, 1996; Department of Energy, 2000):

Table 1.1: Nuclear test explosions by country

Country	Date of first test	Number of tests
USA	July 16, 1945	1030
Soviet Union	August 29, 1949	715
United Kingdom	October 3, 1952	45
France	February 13, 1960	210
China	October 16, 1964	45
India	May 18, 1974	3
Pakistan	May 28, 1998	2
North Korea	October 9, 2006	3
Total		*2053*

Nuclear weapons tests have been carried out in the atmosphere, underwater and underground. The majority of nuclear tests, 1502, have been conducted underground, including all nuclear tests since 1980. Underground testing has evolved into a well-established technique since the first underground test in 1951, when the US test "Buster-Jangle Uncle" detonated in a 5 m deep hole. In the majority of tests, the device is either placed in a tunnel that leads into a mountain or hill, or in a deep borehole into the flat ground. At firing time, nuclear weapons can create pressures up to several 100,000 *bar* and Temperatures of about 10^8 Kelvin (U.S. Congress, Office of Technology Assessment, 1989; Glasstone and Dolan, 1977). Estimation calculations indicate that underground nuclear explosions immediately vaporize approximately 70 metric tons and melt 700 metric tons of rock for each kiloton of explosive yield (Olsen, 1967). This results in underground cavities of melted rock. As soon as the cavity and the surrounding rock cools down, the melt flows down its walls and overlying rock begins to fall down. The cooling process continues for hours to days after the explosion until overlying rock is either strong enough to support the overburden or the cavity collapses in itself, forming a subsidence crater. An intact cavity can effectively trap radioactive fall-out within itself, which is a major advantage compared to atmospheric tests (Rodean, 1968).

Figure 1.1: Subsidence craters, caused by underground nuclear explosions in the Nevada test site.

Beyond that, the United States and the Soviet Union both had programs to use nuclear devices for civilian purposes (Nordyke, 1998; Department of Energy, 2000). These so-called Peaceful Nuclear Explosions (PNEs) were mainly aimed to explore possible use in deep seismic sounding, stimulate oil and gas recovery, or in excavation applications. The idea was eventually dropped, since PNEs could not justify the involved risks and expenses.

Because it is a powerful means of deterrence, nuclear testing has also been used for political reasons and to demonstrate superior military strength. As an example, the most powerful nuclear test explosion, the three stage Soviet Tsar bomb, had a total explosive yield of 50 Mt. However, such a weapon had very little practical use, since it was too large and heavy to be ever used against an enemy (Khariton and Smirnov, 1993).

The extensive testing of nuclear devices in the early decades has been gradually reduced over time. Progress in nuclear disarmament and non-proliferation is to a large

degree owed to diplomatic efforts and is reflected in international treaties.

1.2 The Comprehensive Nuclear-Test-Ban Treaty

In the early 1950s the nuclear arms race and the nuclear testing of the early cold war quickly gave rise to concerns on both sides. In the United States, the Atomic Energy Commission, denying the adverse health effects of atmospheric testing, was starting to face criticism by the public (Wittner, 1997). Concerns became even more pronounced after the United States "Castle Bravo" nuclear test poisoned civilian inhabitants of the Pacific islands Rongelap, Rongerik and Utirik and the crew of a Japanese fishing boat. One member of the crew died from radiation sickness and many of the islands inhabitants suffered from radiation related long-term diseases (Lessard et al., 1984; Cronkite et al., 1997).

In late 1958, the United States announced, that they would halt nuclear testing for one year if the Soviet Union and the United Kingdom would do likewise. With the aim to make the moratorium permanent, the three powers agreed to start negotiations on a test ban treaty. The following negotiations in Geneva were to a large degree protracted because of continued disputes over the design of a suitable verification regime (Divine, 1978). Against the challenges of negotiations, the moratorium lasted from late 1958 through mid-1961, when the arrangement collapsed under a diplomatic conflict about the status of West Berlin.

It took until after the Cuban Missile Crisis that the Partial Nuclear Test Ban Treaty (PTBT) opened for signature on 5 August 1963. The treaty prohibits all test detonations of nuclear weapons on ground surface, in the atmosphere, under water and in outer space. Underground tests, however, were specifically excluded from the treaty. The PTBT has been signed and ratified by the USA, the Soviet Union (resp. Russia), Great Britain and many other countries. However, the nuclear weapons states France, China and Democratic People's Republic of Korea (DPRK) refused to sign the PTBT.

On 1 July 1968, the Nuclear non-Proliferation Treaty (NPT), was agreed upon. It

4

is the first treaty to limit the spread of nuclear weapons, often summed up in its three pillars: non-proliferation; disarmament; the right to use nuclear technology peacefully. The International Atomic Energy Agency (IAEA) was entrusted with the verification of compliance with the treaty. The NPT is a treaty designed to eliminate illicit proliferation of nuclear weapons technology and disarmament. It aims to maintain the status quo in that it permits nuclear weapons capability only to the nuclear weapons states of 1967: China, France, the United Kingdom, the United States of America and the Soviet Union. Yet four states that have demonstrated or are generally believed to be in possession of nuclear weapons are not part of the treaty: India, Pakistan, Israel and DPRK. The framework of the NPT leaves no room to fit these states into the treaty. Moreover, many non-nuclear weapons state signatories have shown themselves unsatisfied with the progress in nuclear disarmament of the nuclear weapons states. The Iranian ambitions to create national capabilities in nuclear power pose another significant problem for the NPT. Massive international concerns about the Iranian fuel cycle program have put the treaty in jeopardy.

The most restrictive nuclear test ban treaty is the Comprehensive Nuclear-Test-Ban Treaty (CTBT). On 24 September 1996 it was opened for signature. The treaty prohibits all members from any kind of nuclear test explosions, regardless the environment. The CTBT constitutes "an effective measure of nuclear disarmament and non-proliferation in all its aspects contributing to the enhancement of international peace and security"(UNGA, 1996). Even though nuclear testing has proved important for the development of nuclear weapons, it is not a necessity. For example, the design of the nuclear bomb "Little Boy", that has been used against Hiroshima, has never been tested before. However, the prohibition of nuclear testing makes it more difficult for a country to develop advanced nuclear weapons (Perry and Scowcroft, 2009). As of December 2014, the CTBT has been signed by 183 states and ratified by 163. India, Pakistan and DPRK are the most important non-signatory states, since they possess nuclear weapons (CTBTO, 2014).

1.3 Detection of nuclear weapons tests

With any international treaty arises the question of verification. A global verification system of the CTBT thus must have the ability to detect, locate and identify clandestine nuclear weapons tests. On the nexus between technology and diplomacy, a powerful verification regime for the CTBT is being established at the moment. Once fully established, it will add to the deterrence against the conduct of clandestine nuclear tests to ensure that all state parties comply with their contractual obligations.

The verification regime of the CTBT will consist of two key technologies: the International Monitoring System (IMS) and On-Site Inspections (OSIs). The (Provisional) Technical Secretariat ((P)TS) of the Comprehensive Nuclear-Test-Ban Treaty Organization (CTBTO) currently is in charge to build up and establish both verification technologies, in order to have the full verification power once the treaty come into effect.

The monitoring capabilities of the IMS consist of three waveform technologies - seismic, hydroacoustic and infrasound monitoring - and monitoring of atmospheric radioactivity. As of December 2014, about 84% of IMS network facilities have already been installed and certified. In full operation, the IMS will constitute the most powerful and comprehensive monitoring system ever established. It will consist of 170 seismic, 11 hydroacoustic, 60 infrasound and 80 radionuclide stations. Of the 80 radionuclide stations, 40 of which will also have capabilities for noble gas (i.e. radioxenon) measurements. While the waveform technologies offer the ability to detect and locate explosions, only the confirmation of short-lived fission products can prove the nuclear nature of any explosion (De Geer, 1996a).

Atmospheric Transport Modeling (ATM) is a key field of research to interpret IMS radionuclide data (Kalinowski, 2001). Dispersion calculations of radionuclides in the atmosphere form the base of the two most important techniques of ATM: forward modeling and backtracking. While forward modeling shows the plume of a real or assumed release into the future, backtracking identifies most probable areas of release based on current radionuclide observations and atmospheric conditions (Wotawa et al., 2003).

All data of the IMS are constantly transmitted through a Global Communication Infrastructure (GCI) to the International Data Centre (IDC) of the CTBTO in Vienna, Austria. The IDC has the task to collect, process and analyze the data. Through the process of data fusion, the IDC combines information of all components of the IMS. Further, the IDC continuously disseminates data products to the state signatories in the form of bulletins. Additionally, raw IMS data is provided to the National Data Centres (NDCs) of these countries.

An OSI is the ultimate measure in the verification of the treaty. Any state party can request an OSI of a suspicious event, based on information collected by the IMS or by national technical means. Within the six day time frame specified in the treaty, an OSI inspection team and its equipment will then be deployed to the area of regard. The inspection team has the task to gather facts on whether a nuclear explosion has taken place or not. It will therefore apply visual and geophysical techniques to locate and radionuclide sampling and analysis to identify events as nuclear or non-nuclear. The OSI regime especially foresees capabilities to employ radionuclide techniques in the field. Aside the analysis of aerosol-bound particulates, this will include underground gas sampling for noble gas analysis (Carrigan and Sun, 2014).

1.4 Radioxenon as a tool for the detection of underground nuclear explosions

The chemical and biological inertness make xenon, like other noble gases, an ideal probe of processes in the ocean, atmosphere and soil (Staudacher and Allegre, 1982). The colorless and odorless gas has a boiling point of 165 K and a density of 5.9 kg/m^3 at Standard Temperature and Pressure (STP) conditions: 1013.25 $mbar$ and 273.15 K. The concentration of xenon in atmospheric air is constant at (0.087 ± 0.001) ppm (Haynes, 2014). There are seven stable isotopes of xenon: ^{126}Xe, ^{128}Xe, ^{129}Xe, ^{130}Xe, ^{131}Xe, ^{132}Xe and ^{134}Xe. Only eight radioxenon isotopes, respectively isomers have half-lives over six hours. Four of them are neutron-deficient; the other four are neutron-rich fission products

and have therefore been considered as CTBT relevant (De Geer, 2001): ^{131m}Xe, ^{133m}Xe, ^{133}Xe and ^{135}Xe.

The first radioxenon measurements in the atmosphere date back to the year 1944. U.S. airplanes have been used to sample and analyze air above Germany in search of the isotope ^{133}Xe (Ziegler and Jacobson, 1995). Because of its high fission yield and its inertness, ^{133}Xe served as an ideal probe for fission processes that could uncover a covert nuclear weapons program. No traces of such a program have been found.

Atmospheric nuclear test explosions of the past have led to the detections of particulate and gaseous fission products. In the hypothetical event of a treaty violation, the atmospheric test scenario however, is rather unlikely. If a violating state party were to carry out a nuclear explosion covertly, it would most probably attempt to minimize the release of radionuclides. Conducting a test underground or underwater can substantially reduce or eliminate the emission of particle bound fission products (U.S. Congress, Office of Technology Assessment, 1989).

Table 1.2: Independent and cumulative fission yields of the four radioxenon isotopes for neutron induced fast fission of ^{235}U respectively ^{239}Pu

Nuclide	Half-life	Fast fission of ^{235}U		Fast fission of ^{239}Pu	
		Ind. yield [%]	Cum. yield [%]	Ind. yield [%]	Cum. yield [%]
^{131m}Xe	11.9 d	2.41×10^{-7}	4.51×10^{-2}	2.67×10^{-5}	5.43×10^{-2}
^{133m}Xe	2.19 d	4.23×10^{-3}	1.92×10^{-1}	4.65×10^{-2}	2.40×10^{-1}
^{133}Xe	5.24 d	1.46×10^{-3}	6.72	1.58×10^{-2}	6.97
^{135}Xe	9.10 h	1.20×10^{-1}	6.60	6.14×10^{-1}	7.54

In the past, leakages of radioactive noble gases have been reported from underground nuclear test sites in the United States of America and the former Soviet Union (Schoengold et al., 1996; Dubasov, 2010). They can migrate into the atmosphere by three main processes, having different time scales. A poorly contained explosion will lead to an immediate release of particulates and noble gases. Another form of release is the seepage along geological faults and cracks. The third mechanism is barometric pumping. Variations in atmospheric pressure are able to draw out subsoil gases even from well-contained cavities (Auer et al., 1996). Subsoil gas migration has been studied extensively in the Non-Proliferation Experiment conducted in September, 1993. It involved a chemical ex-

plosion of 1 kT equivalent releasing ^{3}He and hexaflouride tracer gases, that have been monitored for a year and a half following the detonation (Carrigan et al., 1996). The data gained from the Non-Proliferation Experiment still serves as valuable input for the development of radionuclide gas migration models.

Radioxenon analysis is a key technology of the IMS, especially after the last three nuclear test explosions that have been carried out by the DPRK in 2006, 2009 and 2013. Although the CTBT was not in effect, the tests offered valuable opportunities to test the verification power of the IMS. All three tests have been conducted underground and the explosions have been detected and located by the IMS seismic network. In case of the test in 2006, elevated levels of ^{133}Xe have been detected three weeks later in Yellowknife, Canada. It was possible to link the radioxenon detection by ATM analysis and therefore confirm the nuclear nature of the explosion (Saey et al., 2007). Regarding the explosion event of 2009, the IMS was unable to detect any radionuclides linked to the event, including radioxenon isotopes. While the event could have been a large conventional explosion used to create the appearance of progress of DPRK's nuclear weapons program, its nuclear nature has been widely accepted (Medalia, 2010). In 2013, with a more evolved radioxenon monitoring system in place, ^{133}Xe and ^{131m}Xe has been detected in Japan and in Russia shortly after the suspicious explosion event (Ringbom et al., 2014). Again, utilizing ATM dispersion calculations, the explosion was confirmed to be of nuclear origin.

Radioxenon isotopes, if any, are the most likely fission products to be observed by the IMS network in case of an underground nuclear explosion. In a real case scenario of a suspicious underground explosion, radioxenon isotopes might be the only means to disclose a violation of the CTBT (Bjurman et al., 1990; De Geer, 1996b).

1.5 Sources of radioxenon

Regardless of their short half-lives, radioxenon is found in almost every region of the earth. The reason for this global radioxenon background is two-fold. As already discussed, radioxenon isotopes are difficult to contain from dispersion into the atmosphere. Secondly,

radioxenon isotopes are continuously produced in various nuclear facilities. Understanding the global radioxenon background is of key importance to be able to distinguish civil sources of radioxenon from nuclear explosions. Aside of nuclear weapons tests, the primary and continuous sources of radioxenon isotopes in the atmosphere are nuclear power reactors and radiopharmaceutical production facilities. Minor sources are nuclear fuel reprocessing plants, hospitals and research reactors (Saey et al., 2007).

Recent studies have highlighted the impact of radioxenon releases from radiopharmaceutical facilities on the radioxenon background. While nuclear power plants worldwide are estimated to release around 0.74×10^{15} Bq of ^{133}Xe per year into the atmosphere, the radiopharmacoutical facilities emit roughly 11×10^{15} Bq of ^{133}Xe (Saey, 2009; Wotawa et al., 2010). The two largest facilities alone, at Chalk River, Canada (operated by MDS Nordion) and Pelindaba, South Africa (operated by NTP) account for 10×10^{15} Bq of ^{133}Xe. The high activity levels of radiopharmaceutical releases increase the local and global radioxenon background. Moreover, the radioxenon signature of radiopharmaceutical emissions, i.e. the activity ratios of the four radioxenon isotopes, is similar to signatures from nuclear explosion scenarios. By analysis of the activity ratios between at least three detected radioxenon isotopes and under the requisite of one single source, it is in theory possible to discriminate civil sources of radioxenon from nuclear explosions (Kalinowski et al., 2010).

Because of the negative effects on the capability of the IMS radioxenon network and therefore the detectability of a nuclear test, efforts are currently undertaken to reduce the emission from especially radiopharmaceutical facilities (Doll et al., 2014). To this day, radiopharmaceutical facilities and nuclear power reactors are the main sources of atmospheric radioxenon.

1.6 Radioxenon sampling and analysis systems

When the CTBT was opened for signature in 1996, the capabilities for radioxenon monitoring had yet to be developed. In 1999 the International Noble Gas Experiment (INGE)

was launched as an international collaboration on the development of fully automated atmospheric radioxenon sampling and measurement. Four countries decided to develop such systems as a contribution to the CTBTO: USA, Russia, France and Sweden. The respective systems are Automated Radioxenon Sampler/Analyzer (ARSA), Analyzer of Radioactive Isotopes of Xenon (ARIX), Systeme de Prélevement Automatique en Ligne avec l'analyse des radio Xénons (SPALAX) and Swedish Automatic Unit for Noble gas Acquisition (SAUNA) (Bowyer et al., 1996; Dubasov et al., 2005; Fontaine et al., 2004; Ringbom et al., 2003).

The systems have been designed to comply with the main criterion of the Minimum Detectable Concentration (MDC) for ^{133}Xe, which has to be 1 mBq/m^3 or lower for a 24 h period of sampling (Schulze et al., 2000). All systems have been tested as part of the INGE in Freiburg in 2001 and have proven to fulfill the demands of the CTBTO (Auer et al., 2004). Since then the radioxenon monitoring network of the IMS has been endowed with these systems. The performance of the different systems has been observed and because of technical improvements the typical MDCs have been reduced significantly for many detection systems (Auer et al., 2010). In addition to stationary systems, mobile versions of the ARIX and the SAUNA system became available as well as the Transportable Xenon Laboratory (TXL) especially designed for OSI purposes.

All systems feature the possibility to store a sample in a gas-tight archive bottle for re-measurement by a laboratory. Like the systems themselves, the gas compositions of the archive samples differ in regard to carrier gases and amount of stable xenon.

Table 1.3: Archive sample properties of the three most common sampling systems

IMS noble gas system	SPALAX	ARIX	SAUNA
Container volume [cm^3]	300	210	500
Gas volume [ml] @STP	25	6	351
Pressure [kPa] at 20 °C	9.062	3.107	76.341
Composition of gas	30% Xe (7-8 ml)	1.5 ml Xe, 0.5 ml air	1-1.5 ml Xe
	70% N_2	3.5 ml He, 0.5 ml CO_2	350 ml He
Connector	Stäubly RBE06.7250	Vacuum hose	Swagelok QC4

1.7 The role of laboratories

As an integral part of the IMS, the protocol to the treaty contains a provision that a total of 16 laboratories shall provide support to the network of radionuclide monitoring stations. The laboratories shall further be certified by the (P)TS for the analysis of samples from radionuclide monitoring stations (CTBTO, 1996). Each laboratory that becomes certified for a measurement technology - particulate or noble gas (i.e. radioxenon) - will contribute in the quality assurance program of the network. A certified laboratory will, when required, provide additional analysis of samples from particulate or noble gas stations. Laboratory analyses might achieve greater sensitivity for certain radionuclides of interest. Integrated within the GCI, laboratories will send analysis and operational reports to the IDC of the CTBTO.

The Operational Manual for Radionuclide Monitoring and the international Exchange of Radionuclide Data summarizes the purposes of laboratories as follows (CTBTO, 2010): (a) To corroborate the results of the routine analysis of a sample from an International Monitoring System station, in particular to confirm the presence of fission products and/or activation products; (b) To provide more accurate and precise measurements; (c) To clarify the presence or absence of fission products and/or activation products in the case of a suspect or irregular analytical result from a particular station.

Because of their technical expertise, laboratories shall further assist the (P)TS in technical support, quality assurance programs and training and sample measurement. Laboratories will also function as back-up for the measurement capability of the IMS stations, if needed. In addition to that, laboratories shall be able to support OSI missions in performing analyses of samples gathered during on-site inspections.

The Austrian laboratory ATL03 is one of 16 designated laboratories within the IMS network. In 2001 the ATL03 became the first laboratory to be certified for the analysis of aerosol bound radioactivity (particulates) on filter samples. The highly sensitive low-level background gamma ray detection systems Det3 and Det4 have therefore been built up. By December 2014, a total eleven laboratories had already been certified for particulate analysis.

Table 1.4: The 16 designated IMS laboratories as listed in table 2-B of Annex 1 to the treaty protocol.

	State responsible for laboratory	Name and place of laboratory
1	Argentina	National Board of Nuclear Regulation Buenos Aires
2	Australia	Australian Radiation Laboratory Melbourne
3	Austria	Austrian Research Center Seibersdorf
4	Brazil	Institute of Radiation Protection and Dosimetry Rio de Janeiro
5	Canada	Health Canada Ottawa, Ont.
6	China	Beijing
7	Finland	Centre for Radiaton and Nuclear Safety Helsinki
8	France	Atomic Energy Commission Montlhery
9	Israel	Soreq Nuclear Research Centre Yavne
10	Italy	Laboratory of the National Agency for the Protection of the Environment, Rome
11	Japan	Japan Atomic Energy Research Insitute Tokai, Ibaraki
12	New Zealand	National Radiation Laboratory Christchurch
13	Russian Federation	Central Radiation Control Laboratory Special Verification Service, Moscow
14	South Africa	Atomic Energy Corporation Pelindaba
15	United Kingdom	AWE Blacknest Chilton
16	United States of America	McClellan Central Laboratories Sacramento

Analysis of noble gas samples shall be performed by laboratories that prove to be capable to conduct measurements of radioxenon in sample archive bottles. The CTBTO document on the certification of radionuclide laboratories INF.96 sums up the minimum technical requirements for radioxenon laboratory measurements (CTBTO, 2012).

Table 1.5: Minimum technical requirements of the INF.96 (Rev.9) for noble gas laboratories.

Measurement/Property	Specification
Pressure in station archive container	Combined standard uncertainty <0.5 kPa
Memory effect, if applicable	<5%
Xenon volume in the archive container	Combined standard uncertainty <10%
Xenon volume in the measurement cell	Combined standard uncertainty <10%
Xenon Activity & Activity Concentration	
Isotopes	Detection and analysis of all relevant isotopes, ^{131m}Xe, ^{133m}Xe, ^{133}Xe and ^{135}Xe
Minimum detectable activity for ^{133}Xe	5 mBq, for a blank sample within three days
Minimum detectable activity for ^{131m}Xe and ^{133m}Xe	10 mBq for a blank sample within three days
Minimum detectable activity for ^{135}Xe	15 mBq, for a blank sample within three days
Uncertainty for the measurement of activity concentrations of ^{131m}Xe, ^{133}Xe, ^{133m}Xe and ^{135}Xe	The uncertainty of the activity concentration measurement shall not be larger than 15% for a measurement with a statistical uncertainty of less than 3% combined standard uncertainty
Gas Composition (Optional)	List of gases to be determined N_2, O_2, CO_2, Xe, Ar, and common carrier gases

The last three underground nuclear weapons tests highlighted the key role of radioxenon as a treaty verification tool. However, the Quality Assurance / Quality Control (QA/QC) regime supporting the network of radioxenon sampling and measurement stations had and still has not been fully established. Calibration of radioxenon stations and validation of results thus remains a critical issue, especially since radioxenon standards are unavailable in activities low enough to prevent long-lasting interference with the systems' performance. Many of the 16 laboratories, including ATL03, have subsequently started to develop or acquire radioxenon measurement systems.

1.8 History of the radioxenon laboratory at ATL03

In 2001 the Austrian laboratory ATL03 was the first of 16 IMS laboratories to be certified by the CTBTO for radioanalytical measurements of particulates on air filter samples. For that purpose two low-level High Purity Germanium detector (HPGe) gamma detection systems have been built up, which will be described later in more detail (Schwaiger et al., 2002).

Two years later, a research project has been started with the aim to develop capabilities in the analysis of atmospheric radioxenon samples. In 2006 a first manual system for the measurement of stable xenon and the sample transfer from sample bottles into radioxenon measurement cells has been presented (Raith, 2006). In the same work, methods of radioxenon production by neutron irradiation of highly enriched uranium targets has been introduced. Subsequently, a high-resolution beta-gamma coincidence detection system for the analysis of radioxenon has been developed (Furch, 2007; Schroettner et al., 2010).

This work is the result of recent developments starting in June, 2010. It was decided to develop and set up a new and automated system for the measurement of stable xenon and the transfer into radioxenon measurement cells. The analysis of radioxenon shall further be performed by the low-level HPGe gamma detection systems that have already been built up and are readily available. In parallel, new and easily available methods of radioxenon production have been established. In December 2014, the laboratory ATL03 again was the first IMS laboratory to be certified by the CTBTO for the measurement of atmospheric radioxenon samples.

2 Scope of work

The scope of this work was the continuation of research efforts by extending ATL03's capabilities to the analysis of IMS noble gas samples. The laboratory system has to be capable of analyzing archived gas samples from all four our radioxenon sampling and measurement systems (ARIX, ARSA, SAUNA and SPALAX). Its analysis results, i.e. stable xenon and radioxenon content, shall be accurate and precise and bench-marked by intercomparison or proficiency test exercises.

Furthermore, the processing steps and the performance of the system need to be tested and validated. Thus, readily available radioxenon isotopes in suitable activities are of key importance. With the exception of ^{133}Xe, CTBT-relevant radioxenon isotopes are not available commercially. As a consequence, there was a clear need to develop methods of radioxenon production as part of the project.

Therefore, the scope of work can be described as two-fold:

1. A radioxenon laboratory measurement system that fully complies to the requirements of the IMS and subsequent certification of the laboratory by the CTBTO

2. Establishment of techniques for the production of all four CTBT-relevant radioxenon isotopes that allow thorough testing and validation of system performance

The core of the following work is be the design, development and validation of the Austrian Xenon Laboratory (AXeL). AXeL is able to analyze samples of all four radioxenon sampling systems in a semi-automatic way. For that purpose it first has to

determine the amount of stable xenon content. Methods for the sample purification and transfer into suitable measurement are presented. Taking advantage of existing HPGe detector systems at ATL03, the four CTBT-relevant radioxenon isotopes are quantified down to Minimum Detectable Activities of a few mBq/m^3 air equivalent.

AXeL takes part in intercomparison exercises conducted by the CTBTO and provides accurate and precise analysis results on the total xenon content and specific radioxenon activity. The validation of performance of AXeL constitutes the core of this work.

The second part of this work concentrates on radioxenon production methods. Methods for radioxenon isotope production have been developed, that can supply the four radioxenon isotopes in activities suitable for system testing and validation. Radioxenon isotopes therefore need to be separated from non-gaseous and long-lived parent nuclides in order to not contaminate the detection and processing systems. As a means to validate AXeL as an entire system, a method to produce reference gases with well-defined specific activities of ^{133}Xe, the lead nuclide, is presented.

Bring vor, was wahr ist, schreib so, dass es klar
ist und verficht's, bis es mit dir gar ist.

Ludwig Boltzmann

3 The Austrian Xenon Laboratory - AXeL

3.1 Introduction

The Austrian Xenon Laboratory System (AXeL) has been developed in order to re-analyze radioxenon gas samples within the IMS network. AXeL is able to handle samples of all four radioxenon sampling systems operated by the IMS: ARIX, ARSA, SAUNA and SPALAX.

It has been designed in four independent and automated modules. The modular set-up has been chosen because it allows easy troubleshooting and optimization. The four modules are the Neon Marker System (NMS), the Xenon Measurement System (XMS), the Xenon Transfer System (XTS) and the Radioxenon Detection System (RDS).

AXeL analyzes each sample for:

1. Initial archive bottle pressure

2. Total amount of stable xenon in the sample

3. Total amount of stable xenon transferred into the measurement cell

4. The activities of the four radioxenon isotopes of interest

The following chapter provides detailed information on the operating principle of

each module, its range of operation and the uncertainty budget of measurements. Every sample goes through the operational routine of the AXeL system, which can be described as follows:

1. Connection of the sample archive bottle to the NMS

2. Measurement of initial sample archive bottle pressure and injection of the internal standard

3. Connection of the sample archive bottle to the XMS

4. Measurement of stable xenon

5. Connection of the sample archive bottle to the XTS

6. Transfer of xenon from the sample bottle into a gas-tight syringe

7. Connection of the sample archive bottle to the XMS

8. Measurement of transferred stable xenon

9. Injection of the sample into a measurement cell for gamma-spectroscopic analysis

10. Gamma spectrometry at the RDS to determine the activity concentrations of the four radioxenon isotopes

3.2 Methods of analysis

3.2.1 Analysis of stable xenon

In order to calculate specific radioxenon activities, samples firstly need to be analyzed for their total xenon content. The total amount of xenon in a typical sample ranges from $1\ cm^3$ to about $7\ cm^3$ at STP conditions. In environmental monitoring the amount of radioactive xenon is usually negligible compared to the amount of stable xenon. Analysis of the total xenon content is thus referred to as stable xenon analysis. Since xenon is very well mixed in the atmosphere with an abundance of 87 ppb (Haynes, 2014), the total

amount of xenon in a sample further represents the total sample size. A sample with 1 cm^3 of stable xenon content therefore stands for an equivalent of 11.5 m^3 of atmospheric air.

Stable xenon analysis is performed by gas chromatography with a Thermo Trace GC Ultra gas chromatograph and a Thermal Conductivity Detector (TCD). Helium serves as the carrier gas. Xenon has a low thermal conductivity in comparison with helium, which favors the TCD type detector.

Table 3.1: Thermal conductivity of typical sample and carrier gases at 400 K (Haynes, 2014).

Gas	Thermal conductivity [$10^{-3}Wm^{-1}K^{-1}$]
Helium	189.6
Neon	59.9
Xenon	7.2
Nitrogen	32.8
Oxygen	34.0

The operating principle of the TCD is the comparison of the column gas flow to a reference flow. For that reason the carrier gas is split and one part is directed to the Gas Chromatograph (GC) column while the other one serves as the reference flow. A Wheatstone bridge with heat sensitive resistors acts as the sensor. While the detector resistor (or filament) is heated, changes in thermal conductivity of the column effluent will result in a temperature change of the sensing resistor and therefore change its resistance, which subsequently can be measured as the signal.
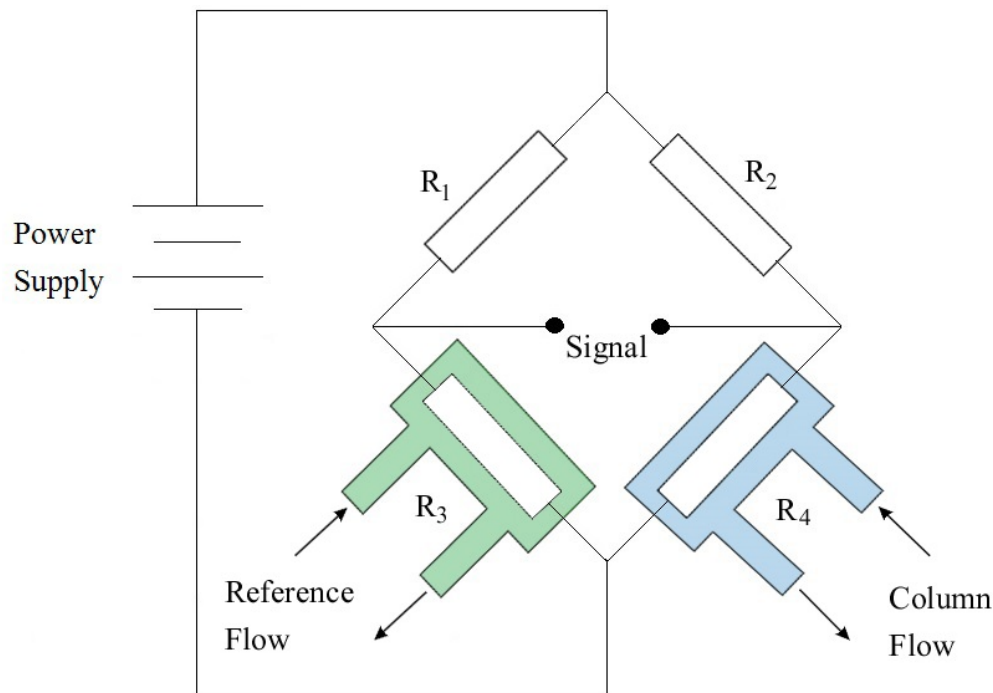
Figure 3.1: Schematic drawing of a TCD detector.

The GC analyzes a sample bottle by taking out an aliquot of the sample into the loop and injecting the aliquot into the column flow. The column is a 1 m long Restek molecular sieve column (part.no.: 88440-800) with a packing of 80/100 and a mesh size of 5 . The oven is set at a constant temperature of 70 $°C$, the detector block is at 75 $°C$ and the filament at 80 $°C$. The TCD is operated in constant voltage mode at 5 V, which offers good linearity over a wide range of operation.

Table 3.2: Parameters for the gas chromatography

Parameter	Value
Carrier gas	Helium
Carrier gas pressure	4 bar
Carrier gas flow	29 mL/min
Column length	1 m
Column inner diameter	2 mm
Column packing	80/100
Mesh size	5
Oven temperature	70 $°C$
Block temperature	75 $°C$
Filament temperature	80 $°C$
Filament voltage	5 V

3.2.2 Analysis of radioxenon

Measurement of radioactive xenon isotopes in the sample is performed through ultra-low-level gamma spectrometry by the use of High Purity Germanium (HPGe) detectors. The four CTBT-relevant radioxenon isotopes emit characteristic gamma radiation during decay.

Table 3.3: Selected gamma emission lines for the four radioxenon isotopes. Data for ^{131m}Xe,^{133m}Xe and ^{133}Xe are taken from the DDEP (Chiste and Be, 2014; Galan, 2012, 2008). Data for ^{135}Xe is taken from the NNDC (Singh et al., 2008).

Isotope	Energy [keV]	Photons per 100 disintegrations
^{131m}Xe	29.46	15.5
	29.78	28.7
	163.93	1.94
^{133m}Xe	29.46	16.0
	29.78	29.7
	233.22	10.2
^{133}Xe	30.63	13.5
	30.97	25.0
	79.6	0.28
	81.0	37.0
^{135}Xe	249.9	90.0

Conceptually, HPGe detectors are reverse-biased diodes. When incident gamma radiation interacts with the detector material, free charge carriers are created in the depletion region, the active volume of the detector, and will be drawn to the respective opposite electrodes. Charge sensitive amplifiers convert the pulse of charge carriers into voltage steps that are further processed by a digital spectrometer. The height of the voltage peak is proportional to the amount of energy, which has been deposited within the active volume by the incident gamma particle. After the analog signal has been converted to a digital signal by an Analog to Digital Converter (ADC), organizing signals according to their pulse height into channels will then give the gamma spectrum. In the gamma spectrum, the basic interaction mechanisms will be visible. Most importantly, this includes the photo peak. Because it contains the information of the total incident energy of the gamma ray, it allows a determination of the radioactive isotope(s) in the sample.

The two detectors (Det3 and Det4) used for this research are Canberra fabricated, planar Broad Energy Germanium detector (BEGe) 5035 detectors. BEGe models cover an energy range from 3 keV to 3 MeV, combined with excellent energy resolution and high efficiencies for typical sample geometries. The two detector crystals are identical in construction. They have nominal diameters of 80 mm and the nominal thicknesses of 34.5 mm, enclosed by aluminium endcaps with carbon epoxy entrance windows. During operation the detectors are constantly being cooled to the working temperature of about 77 K by the use of thermally insulated dewars containing liquid nitrogen.

3.3 The neon marker system

While the four modules generally work separately and independently, the NMS and the XTS share a stainless steel housing and are operated by a Siemens LOGO! 12/24RCo Programmable Logic Controller (PLC). The auxiliary modules Siemens DM16 24R and AM2 RTD have been added to increase the number of output relays respectively allow temperature measurement. The latter is performed by a Pt100 element, which is placed in the xenon trap and used by the XTS. The PLC has been programmed within the Siemens supplied SoftComfort V6.1 software environment. It is connected to the control unit which actuates the valves of the NMS and XTS pneumatically. The user can operate the PLC through the Text Display (TD) which is mounted on the front panel.

In order to measure the total amount of stable xenon in the sample bottle a newly developed method is being applied. A well-known amount of pure neon gas serves as an internal standard, being injected into the sample as the first step of sample processing. Neon has been chosen because it is like xenon a noble gas and therefore has similar chemical properties. Furthermore, neon can easily be separated from xenon by a standard Molecular Sieve (MS) column and be detected by a Thermal Conductivity Detector (TCD). Sample collection and processing at the sampling stations, which includes separation of light and heavy noble gases, make IMS air samples free of neon.
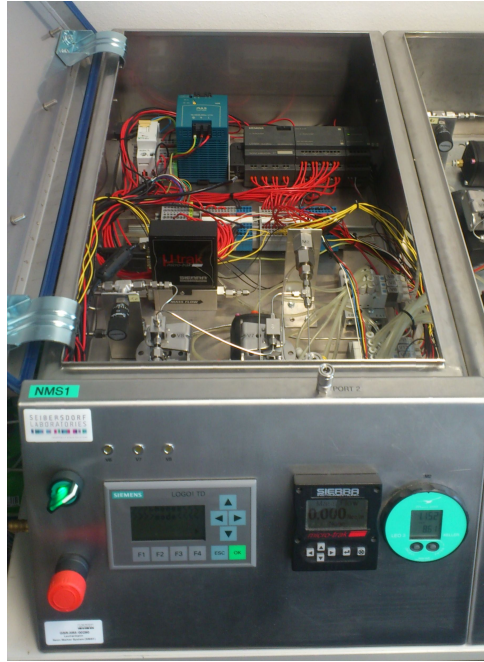
Figure 3.2: The Neon Marker System in its metal casing.

The NMS has been developed to automatically read the initial pressure of the sample bottle and perform the injection of a traceable and precise amount of 5.43 cm^3 of neon into the gas sample. As a first step the pressure of the sample bottle is read on manometer M2 while the valves V6 and V7 are in off-position, respectively closed. Because sample bottles have an under-pressure, the measurement of the initial pressure of the sample bottle allows drawing conclusions about the gas tightness of the bottle and the integrity of the sample. Opening valve V7 will flush helium into the gas line and the sample back into the sample bottle. Helium is being flushed into the sample bottle until the pressure is slightly below atmospheric pressure.

Then, the NMS starts with the injection of neon. It therefore utilizes a Sierra C101 Smart Trak 2 Mass Flow Controller (MFC). Once valve V6 is actuated, neon, which has in the meantime been flowing against the open atmosphere, is led through the MFC into the sample bottle. After one minute of purging and with a constant flow rate of 5.43 cm^3/min, the total amount of neon is reached and valve V6 will be set to off again. At the same time valve V7 is opened and helium is flushed into the sample bottle again, pushing residual neon into the sample bottle. That way, remaining neon in the tubing between valve V6 and the sample bottle is flushed into the gas sample. The helium

flushes facilitate mixing of gases in the sample bottle, as it is injected with 3 *bar* absolute pressure, creating turbulence within the sample bottle.
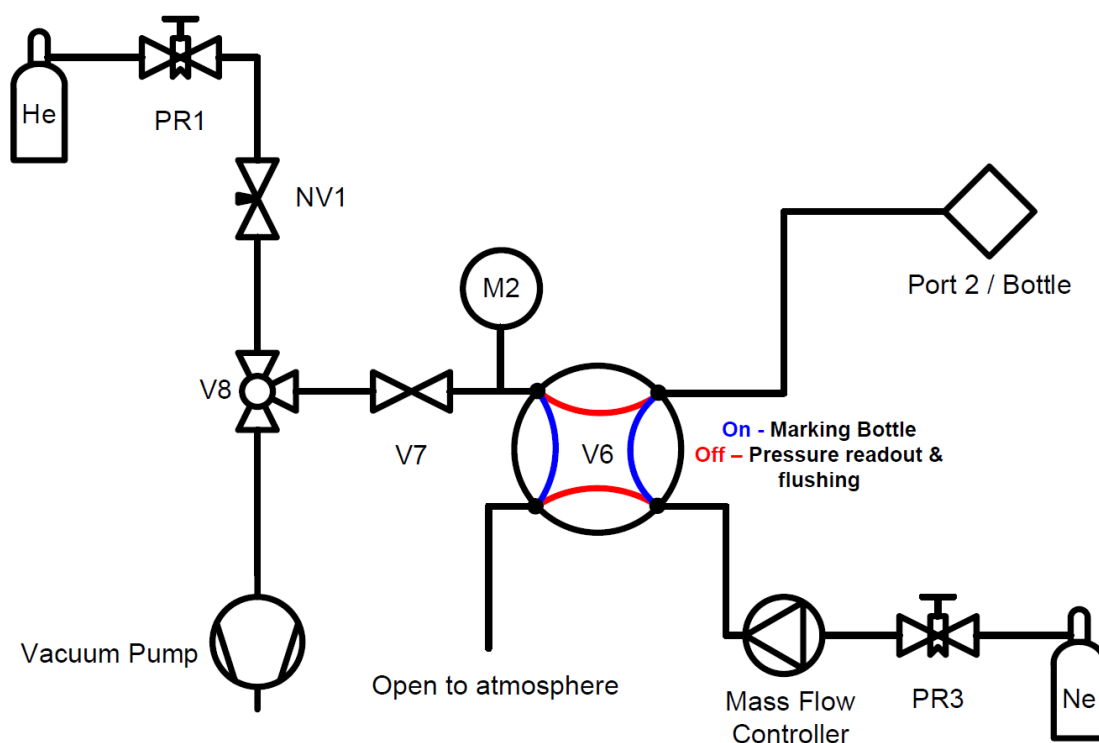
Figure 3.3: The connection scheme of the Neon Marker System.

This procedure creates an internal standard which is used in the further analysis of the sample. The internal standard method allows a precise measurement of the total amount of xenon in the bottle by using the Xenon Measurement System (XMS). A major advantage of this technique is its independence from the bottle volume. IMS bottle types and sizes are not standardized and even for one system type exist different bottle types. Measurements of gas samples in different bottle sizes can thus be performed without relying on information of the total bottle volume. Another advantage is the inherent protection against the consequences of sample loss during processing and analysis. Once the sample bottle is marked, even a substantial loss of the sample would not affect the further analysis of stable xenon. The loss of sample xenon by e.g. incorrect handling of the sample bottles or untight valves would be compensated by the loss of the same amount of neon. The stable xenon analysis would in both cases yield the correct initial

amount of stable xenon. Naturally, however, the lower amount of total sample volume would affect the measurement of radioxenon in terms of acquisition time and Minimum Detectable Activities, even though it would not distort the measurement itself.

3.4 The xenon measurement system

The XMS is operated by a measurement computer, which runs the Thermo Scientific Chrom-Card software Version 2.2. Through the Gas Chromatograph (GC) method, the measurement program, Chrom-Card controls the XMS and its valves and acquires and stores chromatograms. Once calibrated, Chrom-Card is further able to automatically identify and mark peaks, calculate net peak areas and identify peaks based on their retention times.
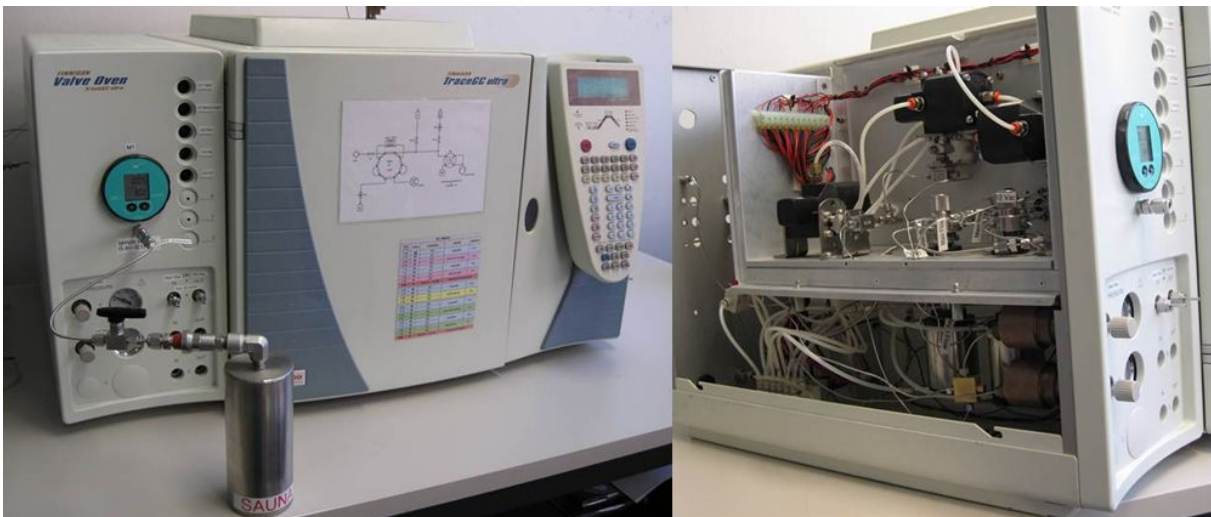
Figure 3.4: Left: A SAUNA archive bottle being analyzed at the XMS. Right: The valve oven of the XMS.

The XMS serves as a versatile instrument for the analysis of gas samples of different volumes and composition. While the methods applied might find application in the analysis of other gases, the current set-up is optimized for the analysis of noble gases, especially neon and xenon. As an integral part of the xenon measurement system (XMS) a Gas Chromatograph (GC) analyzes the sample for its stable gas composition. The automatic routine has been programmed to take a reference gas sample before every sample

measurement and combine both chromatograms into one single readout. The calibration gas consists of 1% of neon and 1% of xenon with the rest being helium. The result is one single readout combining two injections. It typically shows a reference peak of neon, a reference peak of xenon and the neon and xenon peaks of the sample.
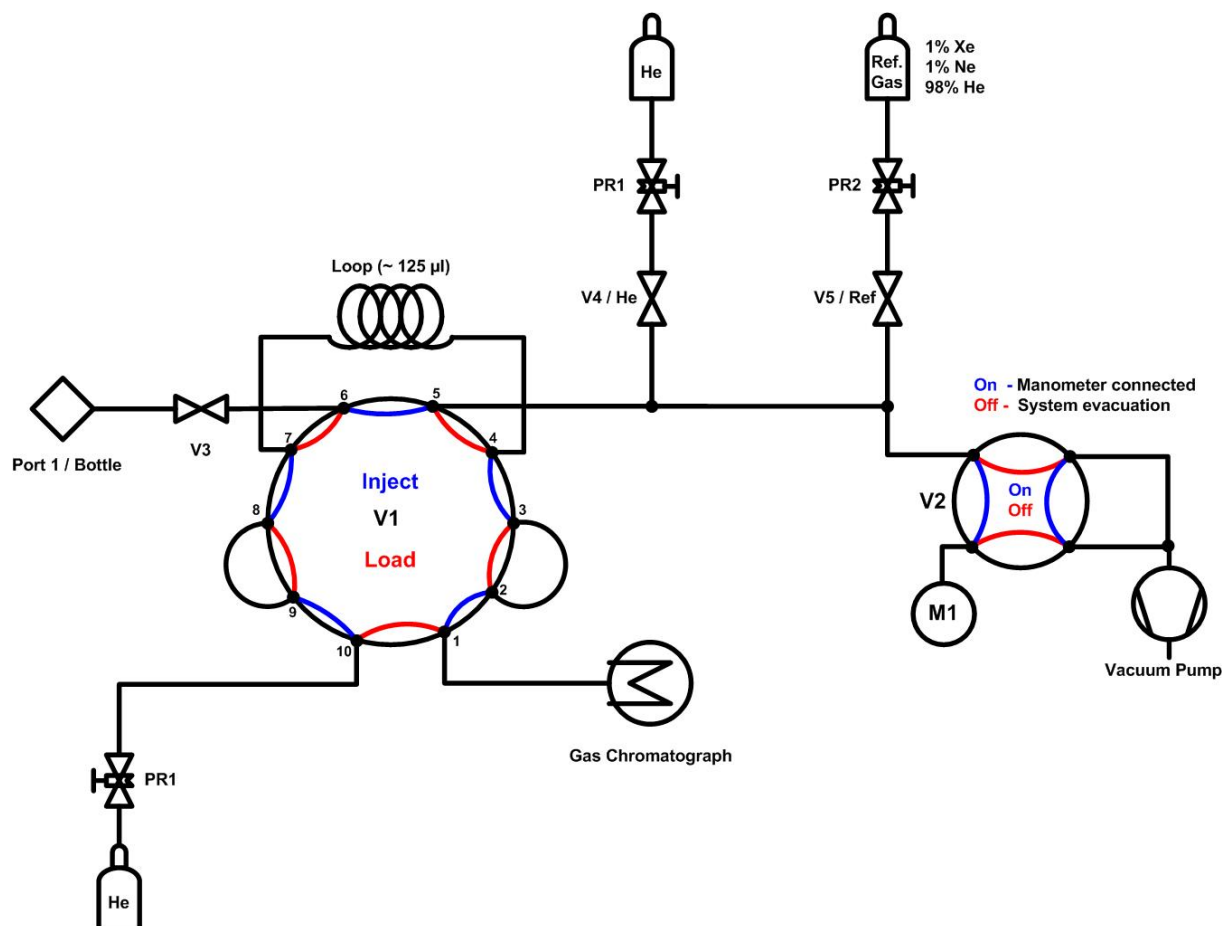
Figure 3.5: The schematic drawing of the XMS.

The XMS is used in two different steps of the sample analysis routine:

1. Determination of the total amount of xenon in a sample bottle

2. Determination of the amount of xenon transferred into a gas-tight syringe

In both cases, the operational routine of the XMS is the same. As a first step, all tubing is evacuated thoroughly. Then, the reference gas fills the 125 μL sampling loop and is directed into carrier gas flow towards the GC column and the TCD, once valve V1 is set to inject. The tubing is cleaned by cycles of helium flushes and evacuation of tubing. At this stage, it is important that the sampling loop is free of residuals of the reference
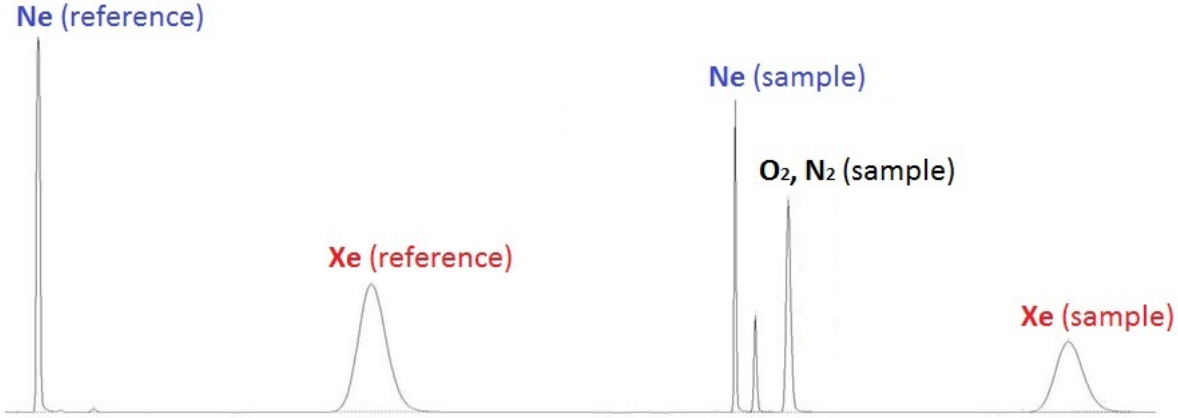
Figure 3.6: Typical reference (left) and sample chromatogram (right), combined into one single readout.

gas. Opening valve V3 will take an aliquot of the sample into the sampling loop. The aliquot is then injected by V1 into the carrier gas flow and directed to the GC column and the TCD for separation and measurement. As a last step, the tubing is evacuated again.

Determination of xenon in the sample bottle is performed by the application of the internal standard technique. The total amount of stable xenon at standard temperature and pressure $V_{STP,Xe}$ is calculated by the following formula:

$$V_{STP,Xe} = \frac{A_{Sample,Xe} \cdot A_{Ref,Ne} \cdot K_{Ref,Ne}}{A_{Sample,Ne} \cdot A_{Ref,Xe} \cdot K_{Ref,Xe}} \cdot V_{STP,Ne} \tag{3.1}$$

$V_{STP,Xe}$ ... STP volume of xenon in cm^3

$A_{Sample,Xe}$ ... Xenon peak area in the sample

$A_{Sample,Ne}$ ... Nenon peak area in the sample

$A_{Ref,Xe}$ ... Xenon peak area in the reference gas

$A_{Ref,Ne}$ ... Nenon peak area in the reference gas

$K_{Ref,Xe}$ ... Xenon concentration in the reference gas (1%)

$K_{Ref,Ne}$ ... Nenon concentration in the reference gas (1%)

$V_{STP,Ne}$ ... Total STP volume of internal neon standard (5.43 cm^3)

As can be seen, the resulting formula is free of parameters of ambient conditions. This is another advantage of the internal standard technique in combination with reference

Table 3.4: The XMS operational routine of sample measurement.

XMS - Method

Time [min]	Valve	Command	Activity	Duration [s]
0	#2	Off	evacuate	42
0.7	#2	On		
0.8	#5	On	flush with	6
0.9	#5	Off	ref. gas to 2 *bar*	
1	#2	Off	evacuate	42
1.7	#2	On		
1.8	#5	On	load	6
1.9	#5	Off	ref. gas to 2 *bar*	
2	#1	Inject for 1 minute	Reference Chromatogram	
4	#2	Off	evacuate	42
4.7	#2	On		
4.8	#4	On	flush with He	6
4.9	#4	Off		
6	#2	Off	evacuate	42
6.7	#2	On		
6.8	#3	On	flush with sample	6
6.9	#3	Off		
7	#2	Off	evacuate	42
7.7	#2	On		
7.8	#3	On	load sample	6
7.9	#3	Off		
8	#1	Inject for 1 minute	Sample Chromatogram	

gases. As ambient conditions affect both, the measurement of the reference gas and the sample, their effect cancels out and the result is a relatively simple comparison of net peak areas. With the GC set-up as described above, the separation of peaks and the determination of net areas is uncomplicated, given that the differences in retention times are large. Since two injections are combined into one readout, the reference gas components appear at the retention times as given below while the sample gas components lag behind the difference of six minutes.

Table 3.5: Retention times of notable gases at the GC set-up.

Retention time [s]	Peak Name
10	Auto Zero
131	Neon
141	Oxygen (possible contaminant)
150	Nitrogen (possible contaminant)
257	Xenon

The relative uncertainty of the xenon volume in the sample bottle, $\sigma_{V_{STP,Xe}}$, is calculated by using standard error propagation. The uncertainties of reference gas fractions of xenon and neon are 2%. The uncertainty of $V_{STP,Ne}$ amounts to 1% according to the certificate of the MFC. The ratio of the neon peak areas amounts shows an uncertainty of 1.5% including variations in atmospheric pressure during marking. The ratio of the xenon peak areas are subject to an uncertainty of about 1% due to automatic peak analysis.

$$\sigma_{V_{STP,Xe}} = \sqrt{0.02^2 + 0.02^2 + 0.015^2 + 0.01^2 + 0.01^2} = 0.035 \tag{3.2}$$

After the transfer of the sample into a gas-tight syringe, the transferred amount of xenon needs to be quantified. Again, the XMS is used for this purpose. This time, however, the internal standard is invalid, due to different adsorption and desorption characteristics of neon and xenon on the active charcoal tram of the XTS.

Figure 3.7: The gas-tight syringe and the plunger holder.

The volume of the gas tight syringe V_{Syr} and the transfer factor from the syringe to

the measurement cell C_{Trans} have been well determined. The amount of xenon transferred into the measurement cell $V_{STP,Xe,MC}$ can thus be calculated by following formula:

$$V_{STP,Xe,MC} = \frac{A_{Sample,Xe}}{A_{Ref,Xe}} \cdot K_{Ref,Xe} \cdot V_{Syr} \cdot C_{Trans} \cdot \frac{p_{Ref} \cdot 273.15}{1013.25 \cdot T_{Bottle}} \quad (3.3)$$

$V_{STP,Xe,MC}$ ... STP volume of xenon in the measurement cell in cm^3

$A_{Sample,Xe}$ ... Xenon peak area in the sample

$A_{Ref,Xe}$ ... Xenon peak area in the reference gas

$K_{Ref,Xe}$ ... Xenon concentration in the reference gas (1%)

V_{Syr} ... Volume of the gas-tight syringe (50.5 cm^3)

C_{Trans} ... Transfer factor from syringe to measurement cell (96.6%)

p_{Ref} ... Pressure of the reference gas in $mbar$

T_{Bottle} ... Temperature of the sample bottle in K

Again, the relative uncertainty of xenon volume in the measurement cell, $\sigma_{V_{STP,Xe,MC}}$, is calculated using standard error propagation. The ratio of xenon peak areas has a 1% uncertainty and the reference gas fraction of xenon itself has a 2% uncertainty. The volume of the syringe has an uncertainty of 1.4%. The transfer factor from the syringe to the measurement cell C_{Trans} has a relative uncertainty of below 0.5%. The manometer M1 (Keller Leo 3) has a total uncertainty of 4 $mbar$. Considering a typical reference gas pressure of 1900 $mbar$, it is 0.2%. Because of handling of the syringe can involve transfer of body heat to the syringe, the uncertainty of the temperature measurement was conservatively estimated to be 1%.

$$\sigma_{V_{(STP,Xe,MC)}} = \sqrt{0.02^2 + 0.014^2 + 0.01^2 + 0.01^2 + 0.005^2 + 0.002^2} = 0.029 \quad (3.4)$$

Stable xenon analysis of the initial sample bottle is performed by using an internal standard of neon. The resulting measurement uncertainty amounts to 3.6%. The transferred amount of xenon within the gas-tight sample syringe relies on the well known volume of the syringe and the reference gas pressure instead. The method yields a total

measurement uncertainty of 2.9%.

3.5 The xenon transfer system

The xenon of the sample bottle needs to be transferred into a measurement cell which is suitable for gamma spectrometry. The XTS has therefore been developed to automatically carry out this task. The transfer is carried out from the sample bottle into a previously evacuated, gas-tight syringe. The syringe is kept at 50 cm^3 by a plunger lock. The amount of transferred xenon can then be measured by the XMS in a second step. Finally, the sample is transferred from the syringe into the measurement cell.

The core of the XTS is a xenon trap based on adsorption on activated charcoal at low temperatures. The trap consists of a circular Carbon Molecular Sieve (CMS) column and a cylindrical copper body surrounding the column inside and outside as to create a large contact surface. The copper body can be heated by an electrical heating element and cooled by liquid or gaseous nitrogen through a PTFE connection hose. The column has a 80/100 packing, an inner diameter of 2.2 mm and a length of 1.8 m.
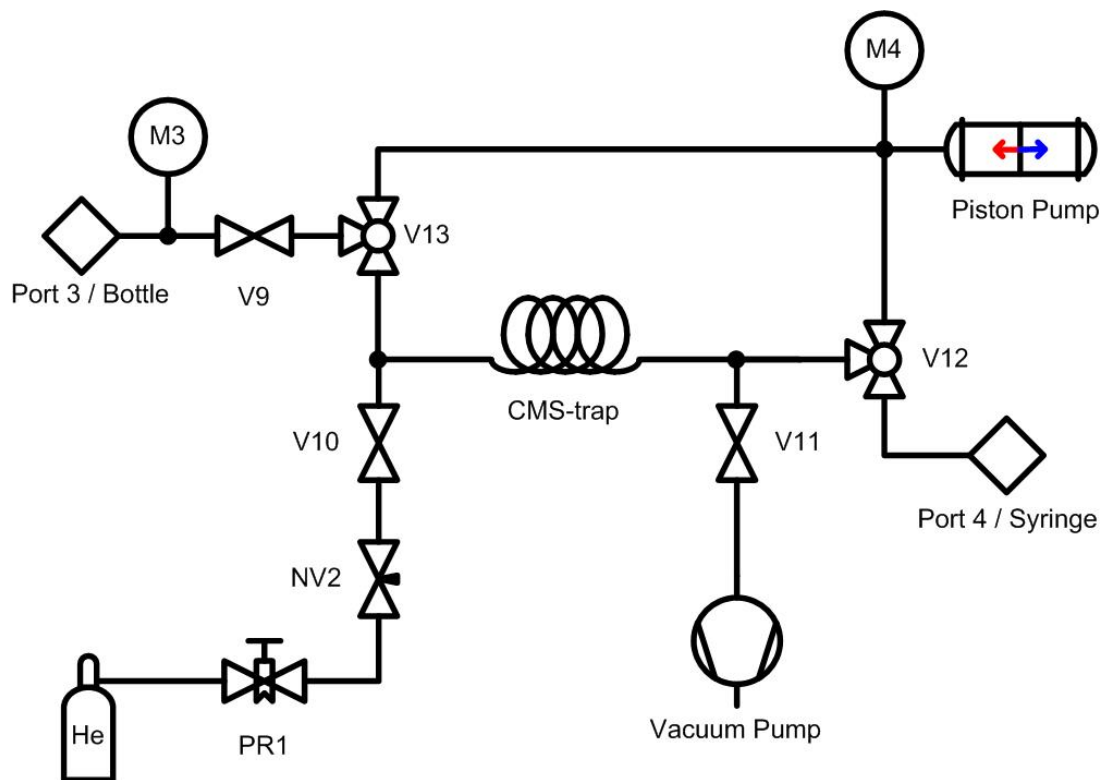
Figure 3.8: The schematic drawing of the XTS.

As a first step, XTS tubing is being evacuated while the trap heats up to 150 °C. After the trap and the tubing has been cleaned, the trap is cooled by cold nitrogen to around 10 °C. Cold, gaseous nitrogen (77 K) is readily available in the laboratory, as detectors need to be filled regularly with liquid nitrogen. The liquid nitrogen dewars that are used for that purpose also have gas outlet valves, that can be connected to the XTS. While the trap is being cooled to 10 °C, the 500 cm^3 piston pump repeatedly sucks in sample gas and then pushes it through the trap. Xenon is being adsorbed in the trap. The temperature of 10 °C is a compromise between adsorption of xenon at active charcoal and undesired adsorption of other gases, mainly nitrogen. The trap is again heated to 150 °C and xenon is released and flushed with short pulses of helium into the syringe. The syringe now contains a mixture of xenon and helium. The three-way valve V12 then closes the syringe off to prevent loss of the sample. As a final step, the tubing of the XTS is evacuated. After each transfer, the syringe and the archive bottle are disconnected. The XTS then performs a post-run cleaning procedure, evacuating all tubing and dead volumes of remains of the sample.

34

After a successful transfer, the syringe is analyzed for the amount of stable xenon at the XMS. The stable xenon analysis of the transferred sample is necessary, since transfer efficiencies depend on the individual gas composition of the sample and the total amount of xenon. Once the amount of transferred xenon has been measured, the syringe is connected to a previously evacuated measurement cell. The transfer from the syringe into the measurement cell is performed manually. The syringe valve is opened so that the sample can flow into the measurement cell. Removing the plunger lock will already move the plunger to the bottom because of the under-pressure in the syringe volume. After disconnection and removal of the syringe, the measurement cell is ready for radioxenon measurement.

3.6 Detection of radioxenon

3.6.1 Gamma spectrometry of radioxenon

Gamma spectrometry of radioxenon is the last step in the analysis and it is performed with two separate HPGe detector systems, Detector 3 (Det3) and Detector 4 (Det4). Both detectors are planar Broad Energy Germanium (BEGe) detectors of the type BE5035 of Canberra. The detector crystals have cross-sectional areas of 5000 mm^2 and thicknesses of 35 mm. The BEGe design combines high efficiency for energies below 1 MeV with good resolution and peak shape over the entire spectrum. In addition to that, the shape of the crystal makes it more transparent to high energy cosmogenic background radiation compared to coaxial detectors. Thus, BEGe detectors exhibit lower background levels than coaxial detectors especially in above ground laboratories such as ATL03.

Ortec DSPEC+ digital spectrometers are used for high voltage supply and signal processing. Spectra are acquired and analyzed by using the software Interwinner 5.0. InterWinner is a universal nuclear spectrometry control and analysis tool. It provides control over all relevant set-up parameters and offers the possibility to define automatic analysis routines in subprograms.

3.6.2 Detector shielding

A low-background environment has been created for the detector systems. The laboratory is placed in a room with 30 cm concrete walls. In the room stands a 2 m x 3 m iron castle of 5 cm thickness. The detectors are placed in sandwich-type shielding constructions. While Canberra's 747E lead shield has been used for Det3, a custom made shielding has been built up for Det4. A hollow, cubically formed, lead shield of 13 cm thickness forms the first passive layer. The lead has a purity of less than 130 Bq/kg of ^{210}Pb. It is followed by 10 cm of borated paraffin, which serves as a neutron moderator and neutron absorber for spallation induced neutrons in lead. The detector chamber has a 2 cm high purity lead plate casing with less than 20 Bq/kg of ^{210}Pb. The innermost layer consists of 4 mm pure electrolytic copper.

Figure 3.9: A radioxenon measurement cell on the detector Det4.

In addition to the passive shielding, both detectors are equipped with active veto shielding. Both active veto systems consist of five plastic scintillator plates, which surround the detector housing on its top and the four sides. Operation in anticoincidence mode significantly reduces background counts from cosmic muon spallation reactions.

Through the combination of passive and active shielding, the total background count rate from 40 keV to 2700 keV amounts to 0.18 counts $s^{-1}kg^{-1}$ (Ge) on Det4 (Schwaiger et al., 2002).

3.6.3 Measurement geometry

There have been three generations of measurement cells in use. The first generation of measurement cells consisted of a cylindrical main body of copper, a carbon window and two O-rings. In addition to that copper ring was mounted onto the main body to fix the carbon window in between the two O-rings. That way it created a cylindrical active volume with a diameter of 76 mm, a height of 3 mm and a total volume of 13.6 cm^3. Due to its memory effect of about 3.5% it has been replaced by the second generation in September 2011. Residual radioxenon mainly has been found in the carbon window as well as in the silicon O-rings. To prevent adsorption of xenon, the material of the O-rings has been changed and the carbon window has been coated with a (2.0 ± 0.5) μm aluminium layer. The attenuation at 30 keV due to the aluminium has been found to be below 0.1% and has been neglected in the efficiency calibration. However, during long-term gamma spectroscopic measurements of radioxenon samples, the effect of a decreasing efficiency has been observed. This is due to adsorption of xenon in the O-ring, which has been observed trap xenon. Due to the large diameter of the O-rings (110 mm) and the copper ring that compresses the o-ring onto the measurement cell body, the detector efficiency of radioxenon at that location is low. Thus, a lower overall efficiency has been observed especially with measurement times of several days. Without quantifying the effect, an improved measurement cell design has been developed.
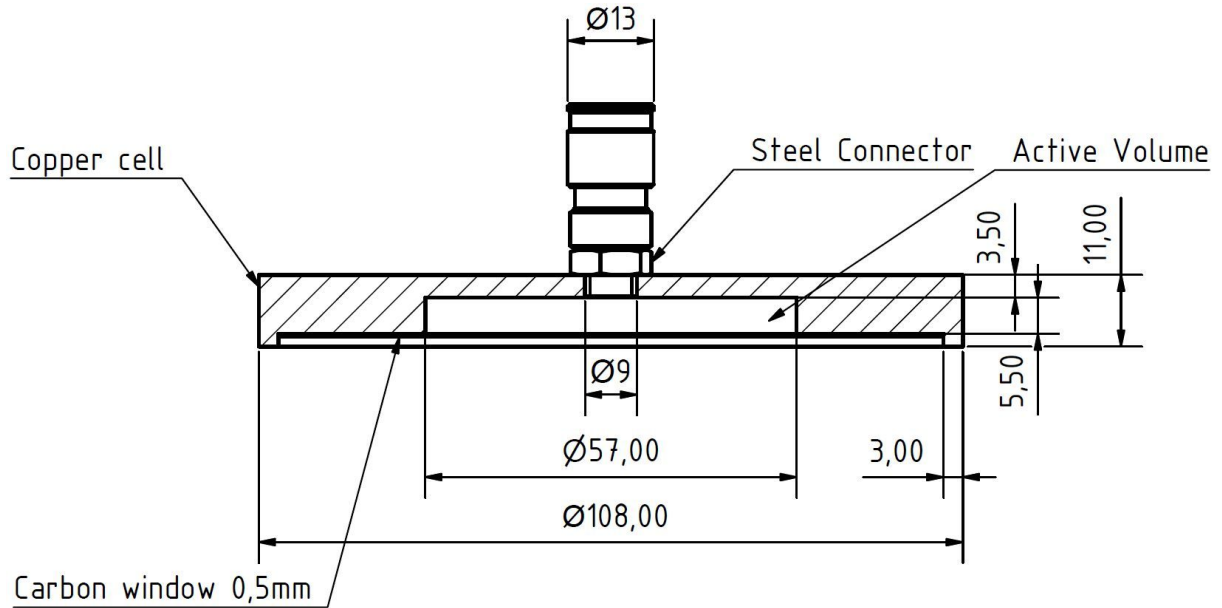
Figure 3.10: Technical drawing of the latest generation of radioxenon measurement cells.

By November 2013, the third generation of measurement cells has been introduced. The active volume has been optimized in terms of efficiency and total volume. The diameter of 57 mm and height of 5.5 mm yield a total volume of 14.1 cm^3. Most importantly, the third generation completely omits the use of o-rings. The aluminium coated carbon window is glued onto the copper main body and compressed at 40 t weight equivalent. The adhesive joint area exposed to the gas sample is kept to a minimum.
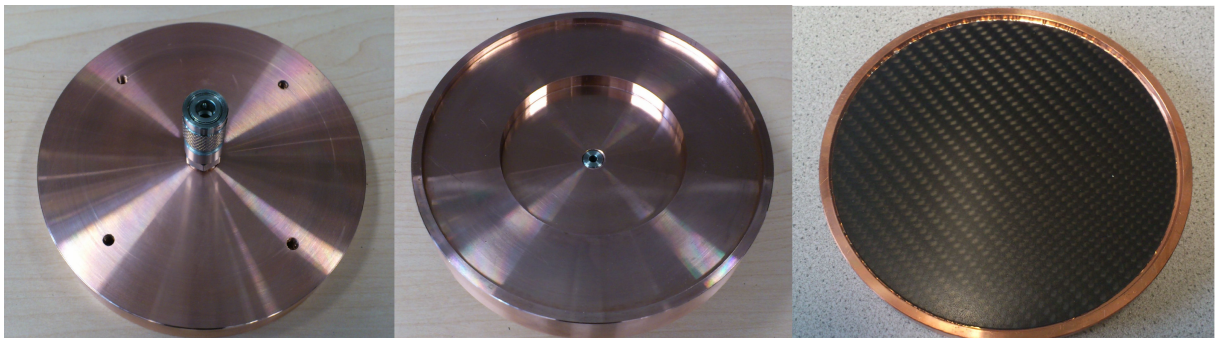
Figure 3.11: A radioxenon measurement cell from the top (left), its active gas volume (middle) and with the carbon window (right).

3.6.4 Energy calibration

Energy calibration is performed with certified reference sources: ^{210}Pb ($46.54\ keV$), ^{241}Am ($59.54\ keV$), ^{137}Cs ($661.7\ keV$) and ^{60}Co ($1173\ keV$, $1332keV$ and $2505\ keV$). Every 24 hours the fine gain is adjusted automatically in order to compensate for energy drift. Therefore the running acquisition is stopped and the spectrum saved for later continuation of the acquisition. A ^{60}Co source is then automatically placed into the detector shielding in close vicinity to the detector by a transport system based on pressurized air. The acquired spectrum allows a software routine to adjust the fine gain of the energy calibration if necessary.

3.6.5 Efficiency calibration

Both detectors have been LabSOCS characterized by the Canberra. The Laboratory Sourceless Calibration Software (LabSOCS) is a physics modeling code based on Monte Carlo N-Particle transport (MCNP). The LabSOCS code simulates detector responses to incident gamma rays coming from point-like or distributed radioactive sources.

Therefore, the detector first needs to undergo a LabSOCS characterization process in which the MCNP model is applied to the detector. Experimental validation of the model is performed by the measurement of point-like sources at various locations around the detector. Experimental validation includes calibration sources of ^{241}Am and ^{152}Eu, covering the energy range from $59.5\ keV$ to $1408\ keV$. The final product is a detector characterization file, containing the response function of the detector to point-like sources in arbitrary geometries. Through parabolic interpolation, the response functions are extended to any arbitrary energy covering the detector's entire energy range. Based on the response functions, LabSOCS is able to generate efficiency curves for distributed sources including self absorption effects. Canberra states typical agreement between model and measurement of about 5% for point-like sources and of about 10-15% for distributed sources and at low energies.
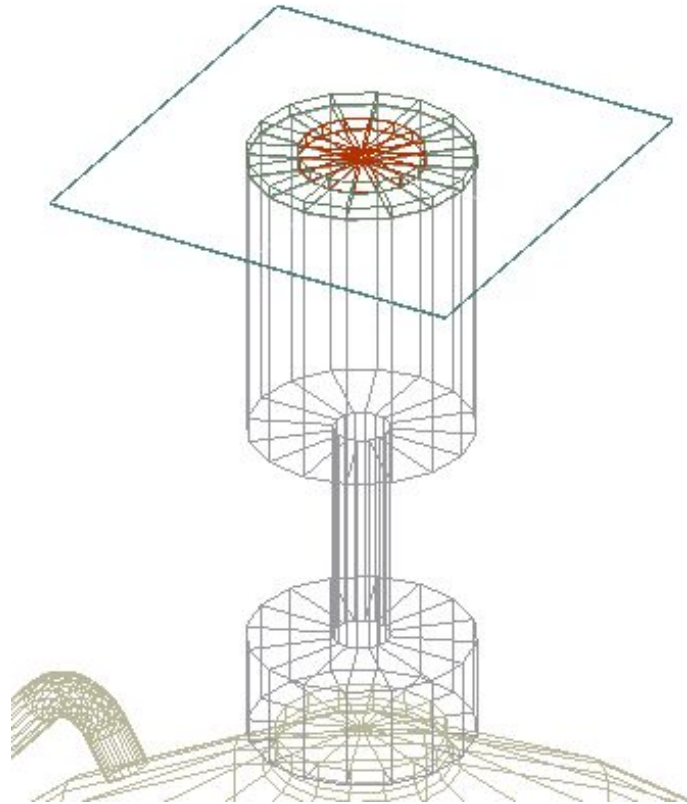
Figure 3.12: Wireframe model of the LabSOCS simulated measurement cell geometry. The active volume is in red color.

Monte Carlo based software algorithms are commonly used to simulate detector-sample geometries and calculate efficiencies. The versatility of these methods allow them to be easily applied to various sample sizes and forms. LabSOCS simulations of the radioxenon measurement cell have been performed to gain the respective efficiency calibration curves.

3.6.6 The minimum detectable activity

In the analysis of an actual measurement a decision criteria is needed to distinguish if a signal is present or not. Especially in low level counting the analyst will face the problem, that the measured gross count within a Region Of Interest (ROI) comes close to the true mean of the background. To tackle this problem a concept of critical limits L_C, and detection limits L_D, has been introduced by LLoyd Currie in 1968 (Currie, 1968). The

concept is build on the requisite that both, the background and the gross counts within a ROI, follow a Gaussian distribution.

L_C is used to determine if a signal was present it a measurement and it is determined after the acquisition. L_D, however, describes the measurement as such, especially its sensitivity for a certain ROI (De Geer, 2004). The Minimum Detectable Activity (MDA) is defined as the smallest amount of activity which is distinguishable from the background. Naturally it is closely related to L_D, however it takes into account sample specific parameters. The MDA is the main criterion to quantify the system sensitivity and therefore the MDA calculation has been standardized (NORM, 2011). However, there is a probability to falsely decide that a line is present, when in fact it is not (Type I error) and the probability to falsely determine a line to be absent when in fact it is present (Type II error). Both cases introduce risks that correspond to fractiles of the Gauss distributions. For the following calculation of the MDA a 5% risk of type I errors and a 5% risk of type II errors is taken into account.

Table 3.6: Radionuclide data for MDA calculation (Chiste and Be, 2014; Galan, 2012, 2008; Singh et al., 2008)

Parameter	^{131m}Xe	^{133}Xe	^{133m}Xe	^{135}Xe
Source	DDEP	DDEP	DDEP	NNDC
Half-life [days]	11.93	5.247	2.198	0.381
Energy [keV]	29.7	30.9	29.7	249.8
Emission probability [%]	44.2	38.5	45.7	90.0

For the 250 keV region, the Full Width at Half Maximum (FWHM) has determined from calibration source by using the ^{113}Sn peak at 255 keV. To consider the Lorentzian shape of x-rays, ^{131m}Xe has been used for the x-ray region. If available, nuclear data has been taken from the Decay Data Evaluation Project (DDEP) (Chiste and Be, 2014; Galan, 2012, 2008). Since the DDEP does not provide data on ^{135}Xe, the National Nuclear Data Center (NNDC) of Brookhaven National Laboratory has been used alternatively (Singh et al., 2008). Starting from the L_C, the MDAs of both detector systems can then be calculated according to following formulas:

$$L_C = k\sqrt{\mu_B\left(1 + \frac{1}{m}\right)} \tag{3.5}$$

The total amount of background counts within a certain ROI is μ_B. Given a Gaussian distributed expectation value, $\sqrt{\mu_B}$ represents its standard deviation. The sum of the background counts of all channels within a ROI give μ_B:

$$\mu_B = \sum_{i\,\epsilon\,ROI} c_i \tag{3.6}$$

The detection limit is defined as:

$$L_D = k^2 + 2L_C \tag{3.7}$$

The detection limit L_D at a 95% confidence level then is:

$$L_D = 2.71 + 4.65\sqrt{\mu_B} \tag{3.8}$$

The MDA then is:

$$MDA = \frac{L_D}{T \cdot \epsilon_\gamma \cdot S_\gamma \cdot P_\gamma \cdot K_C} \tag{3.9}$$

The decay correction during acquisition time, K_C, is defined as:

$$K_C = \frac{1 - e^{-\lambda_i t_C}}{\lambda_i t_C} \tag{3.10}$$

μ_B ...   true mean of the background signal

m ...   number of background measurements (m=1)

k ...   fractile of the Gaussian distribution

L_C ...   critical limit

L_D ...   detection limit

K_C ...   decay correction during acquisition time

ϵ_γ ...   attenuation corrected efficiency (counts per gamma within ROI)

S_γ ...   correction for true coincidence summing (no corrections applied)

P_γ ...   gamma emission probability (gammas per decay)

λ_i ...   decay constant for the isotope i

t_C ...   clock real time between start and end of acquisition ($t_C \approx$ T)

Table 3.7: Input parameters for Det3 and Det 4.

Det3	Half-life [d]	E [keV]	FWHM [keV]	Start [ch]	End [ch]	μ_B [cpd]	ϵ_γ [%]	P_γ [%]
^{131m}Xe	11.96	29.7	0.69	170	180	174	26.25	44.2
^{133m}Xe	2.198	29.7	0.69	170	180	174	26.25	45.7
^{133}Xe	5.247	30.9	0.69	177	187	171	26.25	38.5
^{135}Xe	0.381	249.8	0.99	1462	1476	213	16.79	90
Det4	Half-life [d]	E [keV]	FWHM [keV]	Start [ch]	End [ch]	μ_B [cpd]	ϵ_γ [%]	P_γ [%]
^{131m}Xe	11.96	29.7	0.65	170	180	29.3	25.1	44.2
^{133m}Xe	2.198	29.7	0.65	170	180	29.3	25.1	45.7
^{133}Xe	5.247	30.9	0.66	177	187	27.7	25.51	38.5
^{135}Xe	0.381	249.8	0.97	1462	1476	30.7	16.03	90

Based on above considerations and according to (CTBTO, 2012) the MDAs are calculated for acquisition times of or within three days and six days.

Table 3.8: MDAs for Det3 and Det4 within three and six days of spectrum acquisition

MDA within 3d	Det3	Det4
^{131m}Xe	3.9 mBq	1.8 mBq
^{133m}Xe	5.4 mBq	2.4 mBq
^{133}Xe	4.9 mBq	2.1 mBq
^{135}Xe	11.5 mBq	4.9 mBq
MDA within 6d	Det3	Det4
^{131m}Xe	3.0 mBq	1.3 mBq
^{133m}Xe	5.3 mBq	2.4 mBq
^{133}Xe	4.1 mBq	1.8 mBq
^{135}Xe	11.5 mBq	4.9 mBq

Figures 3.13 and 3.14 illustrate the MDAs as functions of acquisition time.
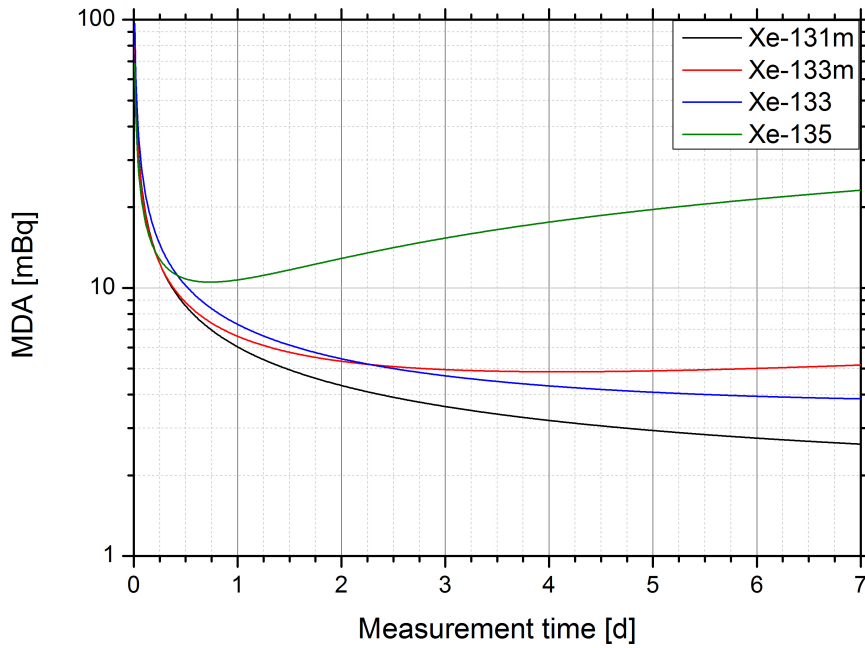
Figure 3.13: The MDA of detector Det3 as a function of measurement time
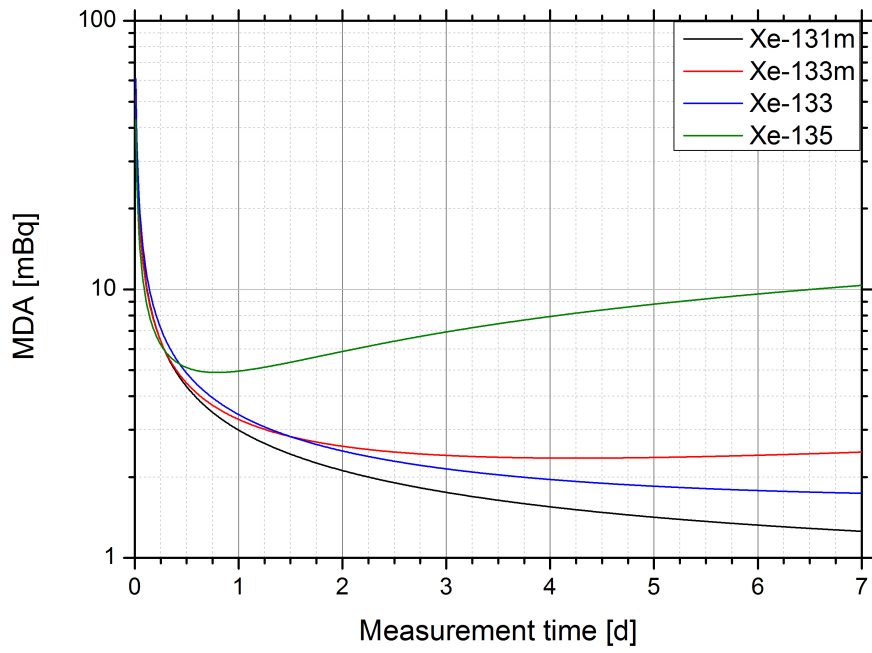
Figure 3.14: The MDA of detector Det4 as a function of measurement time

Si un hombre nuca se contradice,

será porque nuca dice nada.

Miguel de Unamuno

4 Validation of the performance of AXeL

4.1 Validation of the neon marker system

The approach of the NMS relies primarily on the accuracy and precision of the MFC, which needs to be validated. Both characteristics are the main influence on the uncertainty of the stable xenon measurement at a later analysis stage.

As a precondition, sufficient mixing of the internal standard with the sample gas is required for further analysis. Furthermore, since the MFC works against atmospheric pressure during warm-up, the independence from variations in ambient pressure needs to be validated. There are three processes that need to be validated:

1. The accuracy and precision of the MFC is consistent with its specifications

2. The internal standard is well mixed with the sample gas after marking

3. The operation of the NMS is independent of ambient conditions, primarily atmospheric pressure

4.1.1 The mass flow controller

The NMS utilizes a Sierra C101 Smart Trak 2 mass flow controller for the neon injection into the sample bottle. According to the certificate of traceability to the National Institute of Standards and Technology (NIST), the accuracy of the MFC is 1% of full scale. However, experimental testing of the original MFC calibration showed considerable differences between the total amount of injected neon as stated by the MFC compared to measurements on a gas chromatograph. Test runs have been conducted in which a gas bottle of well-known volume has been marked with neon. Gas analysis showed a discrepancy in the total amount of injected neon of about 5% compared to the expected value. A deviation of such magnitude seemed inconsistent with the accuracy of the MFC stated in the certificate. A simple method has therefore been applied to test the MFC and to quantify its absolute accuracy.

The experimental setup is based on a method for volumetric gas measurement. It relies on the displacement of water in an open compensating reservoir. It further consists of a narrow-necked 500 mL volumetric flask and a sufficiently large measuring cup. The volumetric flask is filled up with water and then placed upside down into the measuring cup, which itself contains water. With no remaining air in the volumetric flask, it provides a well-known volume that is filled with water. The MFC is operated at a constant rate of neon and the steel tubing is placed underwater into the measuring cup. The experiment starts once the flowing neon is directed into the measuring cup. By measuring the time needed for the water surface to reach the 500 mL marking, the average mass flow rate can be calculated.

The pressure of the neon gas in the volumetric flask is equal to the ambient air pressure, when the water surfaces in- and outside the volumetric flask are equal. This is achieved by slightly moving the volumetric flask accordingly once the gas volume comes close to the 500 mL marking. Temperature and atmospheric pressure are recorded during the experiment to convert into STP conditions.
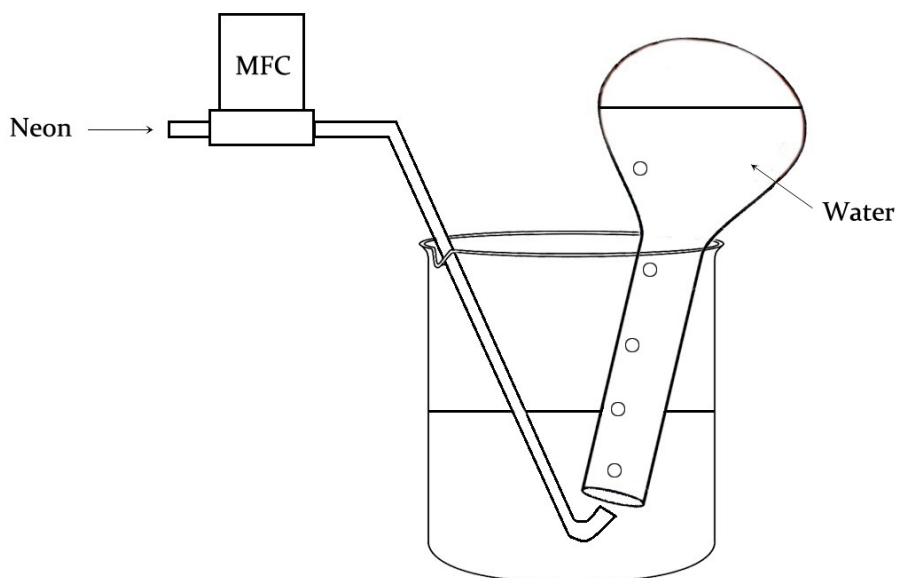
Figure 4.1: A simple method of volumetric gas flow measurement.

During initial tests of the MFC the analysis of marked samples showed systematic discrepancies to the expected values. Due to the discrepancies the MFC has been tested in two testing campaigns.The two tests of the first campaign have shown a difference between measured and stated STP flow of about minus 3%. However, one has to bear in mind the relative humidity of the gas. Since the neon gas elevates through the water in small bubbles and is caught in a relatively small volume, the dry gas becomes humid. Thus, the gas expands taking up a slightly higher volume. This effect, nonetheless, cannot be the reason for the discrepancy, on the contrary; it would certainly lead to a faster fill-up of the 500 ml and to an overestimation of the actual flow. From this result it has been concluded that the actual gas flow is lower than indicated by the MFC.

Based on that, the MFC has been sent back to the manufacturer accompanied with a detailed test report and a kind request for revision and if needed recalibration. The Sierra customer service was very cooperative and a recalibration of the MFC has been carried out. After the recalibration a second testing campaign was started.

Compared to the first campaign, the tests show that the MFC was recalibrated, but a difference in the other direction has been observed. Although the relative humidity in

the gas volume was not recorded during the tests, estimations can be made. Because of the constant bubbling and the small volume, it seems reasonable to assume a relative humidity slightly below or at equilibrium, i.e. between 80% and 100%. For typical room temperatures the saturation vapor pressure of water at different temperatures is (Haynes, 2014):

Table 4.1: Saturation vapor pressure of water at different temperatures.

Temperature [°C]	Saturation vapor pressure [$mbar$]
23.6	29.124
23.8	29.477
24.0	29.833
24.2	30.194
24.4	30.560

Based on these values a correction can be made, which compensates for the higher volume of the neon gas because of its humidity. As can be seen in table 4.2, the first two test runs show the initial deviation of over 5%. Contrary to that, the tests number 3 and 4, which were conducted after recalibration, are consistent with the corrected STP flow. The re-calibrated MFC showed good agreement to the STP flows measured in two test runs. The uncertainty of 1% at full scale stated in the NIST traceable certificate of calibration is therefore reasonable.

Table 4.2: Performance of the Mass Flow Controller before and after recalibration

Test #	Rel. Humidity [%]	Corrected STP Flow [ml/min]	Stated STP Flow [ml/min]	Difference [%]
Test 1	80	3.509	3.7	-5.16
Test 1	100	3.487	3.7	-5.75
Test 2	80	3.501	3.7	-5.39
Test 2	100	3.478	3.7	-5.99
RECALIBRATION				
Test 3	80	5.447	5.43	0.31
Test 3	100	5.413	5.43	-0.32
Test 4	80	5.432	5.43	0.03
Test 4	100	5.399	5.43	-0.57

4.1.2 Mixing of the internal standard with the sample

Sufficient mixing of the internal standard with the sample is an important precondition for further analysis. Estimations which are only considering diffusion will in general underestimate mixing, because of turbulences during marking and flushing of the bottle. An experimental approach was chosen, in which different bottles have been marked with neon and analyzed at different times after the marking. Gas bottles of two noble gas sampling systems (SAUNA and SPALAX) have been prepared and tested in two test runs.

The bottles were filled with a mock mixture of 30% xenon and 70% nitrogen. After marking with neon, the bottles have been analyzed by using the XMS. The experiment aims to test the mixing process only, for that purpose the ratio of xenon to neon is used.

Table 4.3: The results of testing sufficient mixing of the neon internal standard with the sample gas for SAUNA and SPALAX sample gas bottles.

Type	Time after marking [h]	Xe peak area	Ne peak area	Ratio Xe/Ne
SAUNA	0.1	587809	54562	3.824
SAUNA	1	587508	54078	3.871
SAUNA	26	524914	49291	3.805
SAUNA	94	487611	44830	3.883
SPALAX	0.1	554628	83562	2.382
SPALAX	3	538556	80916	2.377
SPALAX	22	520239	78228	2.382

SAUNA and SPALAX archive bottles are different in total volume, resulting in different total amounts of xenon and neon in the sampling loop. While in both cases, the total amount of xenon and neon in the sample decrease, the ratios of xenon to neon do not change significantly over time. This result shows that the prerequisite of sufficient mixing is satisfied, even for short time spans.

4.1.3 Independence of atmospheric pressure

The measurement principle of the MFC is referenced to gas flows in standard conditions, which makes the MFC itself independent of ambient conditions. During warm-up, the

MFC works against atmospheric pressure to stabilize its flow rate. If the gas bottle is at a pressure different than atmospheric pressure, switching on valve V6 will lead to systematic errors. Neon from dead volumes between the MFC and valve V6 will either be sucked into the bottle or pushed back. Thus, this will alter the total amount of injected neon. These effects cancel out when the injection is started slightly below and stopped at slightly above atmospheric pressure.

4.1.4 Reduction of systematic uncertainties

One aim in the design of the instrument and in the operational routine was to minimize systematic uncertainties. First, the volume of the tubing between the MFC and the sample bottle is kept as low as possible ($< 1ml$). Once the NMS is started, the MFC stabilizes itself working against atmospheric pressure, releasing neon into ambient air. Second, during that time the sample bottle is filled up with helium to a pressure of 980 $mbar$. This step is necessary to prevent a falsification of the injected neon amount due to difference in pressure between the MFC output and the sample bottle. The pressure gradient would draw neon gas from the tubing into the sample bottle. The effect cancels out when the pressure differences at the start and the end of the neon injection are equal according to amount.

Therefore the pressure in the sample bottle is brought to a pressure slightly below the yearly average atmospheric pressure of (995 ± 10) $mbar$ at Seibersdorf. Filling-up of the archive bottle is carried out automatically before each neon-marking procedure. Experiments have been performed to evaluate the influence of variations in atmospheric pressure on the amount of injected neon. Neon-free bottles have been marked with neon on days with different atmospheric pressure. To highlight the effect of a variation of atmospheric pressure on the measurement, two days with comparatively low, respectively high atmospheric pressures have been chosen. The bottles have then been analyzed on the XMS.

The variations of the neon sample peak areas at a certain atmospheric pressure amount to about 1% respectively lower. This is in consistency with the uncertainty of the

Table 4.4: Independence of ambient pressure from the amount of injected neon gas.

Atm. Pressure [*mbar*]	Ne(ref) peak area	Ne(sample) peak area	Ratio Ne(ref)/Ne(sample)
986.6	133761	55998	2.389
986.6	134074	55107	2.433
986.4	132086	55271	2.390
1004.3	134186	55421	2.421
1004.2	135132	55402	2.439
1004.2	133699	54516	2.452

MFC. The averaged ratios of a neon reference peak with the neon sample peak however are 2.404 at 986 *mbar* and 2.438 at 1004 *mbar*. The relative deviation is thus less than 1.5%.

4.2 Validation of the xenon measurement system

The XMS uses gas chromatography to analyze a sample for its xenon content. Therefore it takes an aliquot of the sample into the sampling loop and injects it into the column and detector. It can be used either by using an internal neon standard (in case of the sample bottle) or by using the well-known volume of a gas tight syringe. It has been tested and validated for both operation modes. For the internal standard technique, following processes need to be validated, respectively the uncertainties considered:

1. The uncertainties of the reference gas

2. The linearity of the gas chromatograph for the entire range of operation

3. The uncertainty of the gas chromatograph due to noise of the TCD detector output signal and the effects on the automatic peak analysis software

Without an internal standard, these additional sources of uncertainty need to be considered:

1. The uncertainty of the manometer

2. The uncertainty of the syringe volume

3. The uncertainty of the temperature measurement

4.2.1 Reference gases

The reference gas contains 1.01% of neon and 1.01% of xenon with the rest being helium. The respective uncertainties are 2%, stated by the manufacturer providing a certificate traceable to national or international standards.

4.2.2 Gas chromatograph

The GC uses a Thermal Conductivity Detector (TCD) to analyze the components of a gas sample. Before each sample, an automatic calibration is performed by injecting reference gas. The reference gas contains xenon and neon both at suitable concentrations of about 1%. The TCD is operated in a constant voltage mode, which offers a large range of linearity. In addition, the linearity is strongly dependent on the size of the sampling loop, since it directly affects the total amount of xenon being analyzed. By using reference gases of known composition, the linearity of the XMS has been verified for a large range of xenon STP concentration (in the sampling loop). At low STP concentrations the uncertainties of the method become increasingly relevant. Nonetheless, there is no systematic bias visible at very low concentrations. The measurement regime for xenon concentration ranges from 0.06 to 10 $mL(STP)/100\ cm^3$. Within this region the XMS is free of any significant bias.

The validation of linearity has been performed with six reference gas mixtures, including different fractions of xenon: 99.999%, 30.1%, 1.01%, 0.404%, 0.103% and 0.0997%. The systematic uncertainties of the amount of xenon in the reference gas mixtures are respectively: <0.01%, 1%, 2%, 2%, 5% and 2%. Note that the error bars in the figure only show statistical uncertainties of the measurement method.
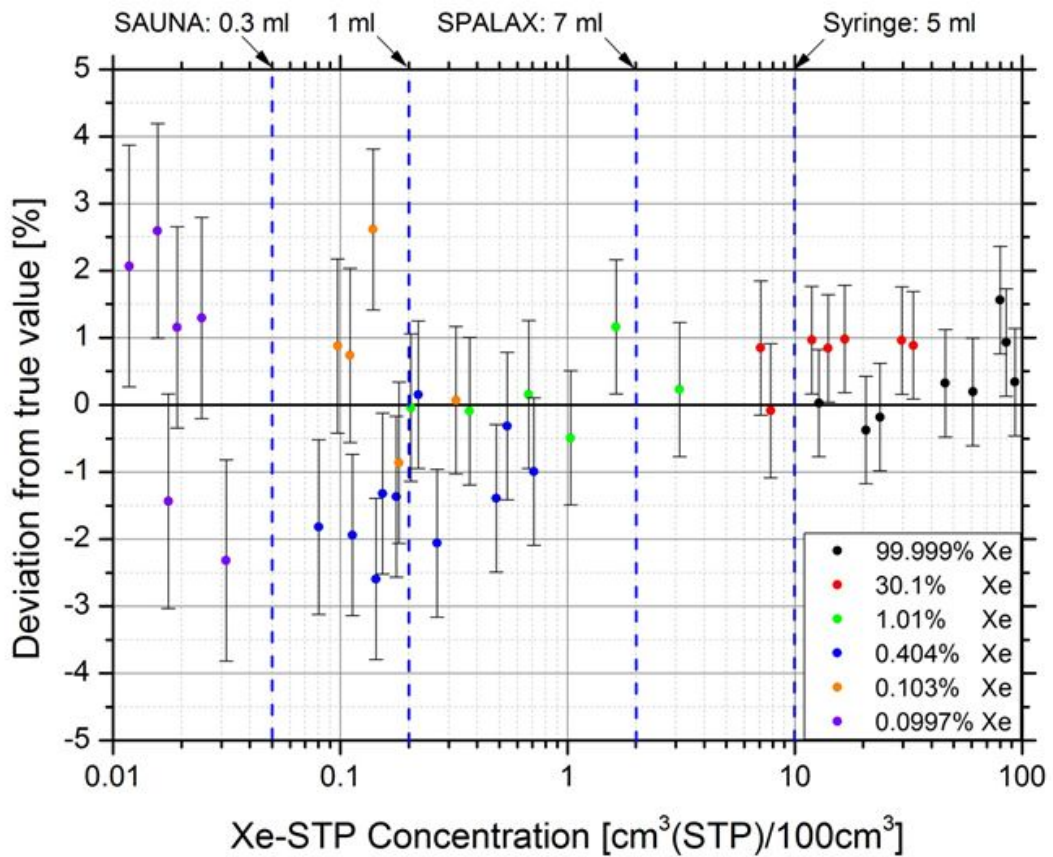
Figure 4.2: Results of the validation of linearity of the stable xenon measurement.

Uncertainties in stable gas analysis arise mainly because of variations in automatic peak analysis. Fluctuations of the TCD can result in slightly different baselines and therefore peak areas. During 104 runs test runs, the effect has been observed by comparing neon and xenon reference peak areas of subsequent chromatograms. The average areas of neon and xenon peaks show a relative statistical uncertainty of 0.68% respectively 0.65%, obtained by experiment. The uncertainty of the ratio of neon or xenon peak areas between sample and reference gas is then about 1%.

$$\sigma_{(V(STP,Xe,MC))} = \sqrt{(0.007^2 + 0.007^2} = 0.98\%$$

4.2.3 Manometers

The manometer type used in the XMS is a Keller Leo 3. The instrument has a typical uncertainty of 0.1% of its full scale (4 *bar*). This amounts to 4 *mbar* of typical total uncertainty. The manometer can be re-calibrated by connecting it to the more precise Keller Lex 1. Lex 1 manometers have a range of operation of 0 to 3 *bar* and typical measurement uncertainties of 0.3 *mbar*. Lex 1 manometers, however, are more delicate than Leo 3 manometers and damageable to pressures exceeding their range of operation. It is therefore only used for re-calibration of the Leo 3 manometers. The Lex 1 manometer at the ATL03 is traceable to international standards according to the certificate of the Deutscher Kalibrierdienst (DKD).

4.2.4 Syringe volume

The syringe volume has been measured gravimetrically. The weight difference between the evacuated syringe and the syringe filled with deionized water has been determined to be 50.33 $g \pm 0.2\%$. Using the density of water of 0.9973 g/cm^3 at 24 $°C$ (Haynes, 2014) and taking into account uncertainties of dead volumes, this leads to a total volume of 50.47 $ml \pm 0.7\%$. Moreover, an additional component of uncertainty has been introduced to compensate for handling of the syringe and the plunger lock. Placing the plunger lock in position can result in variations of up to 1.2% in volume. The resulting uncertainty of about 1.4% has shown good agreement with experiments. The syringe volume of 50.5 $ml \pm 1.4\%$ will thus be used in further calculations.

4.2.5 Temperature measurement

The temperature is being measured by a Thommen HM30 Meteo station. According to its certificate, the device has an uncertainty of measurement of 0.3 K. At room temperature, the uncertainty amounts to 0.1%. Temperature measurement, however, is subject to systematic uncertainties. This is due to the fact, that the ambient air and the gas sample do not necessarily have the same temperature. For example, in case of the

stable xenon measurement within the gas-tight syringe, handling of the syringe can cause a transfer of body heat to the sample gas. In case of the pressure measurement of the gas bottle, the steel container represents a large heat reservoir that can cause differences in ambient and sample gas temperature. Both cases are minimized by measures in the Quality Assurance Program (QAP), like avoiding exposure to body heat. Experimental assessment nevertheless suggests systematic uncertainties of about 1% (3 K).

4.3 Validation of the xenon transfer system

4.3.1 Cross contamination

Dead volume and large surface area are the most important sources of cross contamination. Gases of a sample can reside in dead volumes or adsorb onto surface areas, where they are able to stay until they mix with the next sample. The design of the XMS includes several dead volumes and a large surface area, most of which is the CMS trap. Because of that, before and after every sample transfer the system is being cleaned automatically. This includes baking out of the CMS trap and flushing it with helium as well as flushing and evacuation of dead volumes.

A cross-contamination check (combined with a memory effect test) has been performed. A spike sample, containing all four radioxenon isotopes and 1.01 cm^3 of stable xenon, has been prepared. The spike sample has been processed and analyzed just as any IMS sample. A second mock sample containing also 0.92 cm^3 stable but without any radioactive isotopes xenon has also been prepared and scheduled as a follow-up sample. The follow-up was processed later on the same day. The acquisition times of both samples have been long enough such that the statistical uncertainties of activity in the measurement cells were below 5%. The three nuclides ^{131m}Xe, ^{133}Xe and ^{135}Xe had high enough activities to be useful for testing the cross contamination.

Table 4.5: Results of the cross-contamination test.

Measurement	Stable Xe [cm3]	^{131m}Xe[Bq]	^{133}Xe [Bq]	^{135}Xe [Bq]	Total [Bq]
Spike Sample	1.01	210	300	340	850
Follow up	0.92	0.41	0.63	0.7	1.7
Cross-Contamination [%]:		0.20	0.21	0.21	0.20

The cross contamination between subsequent samples is shown to be 0.21% respectively lower. AXeL therefore fulfills the technical requirement of less than 0.3% cross contamination detailed in (CTBTO, 2012). As a quality assurance measure, the cross contamination factor of the XTS is checked periodically.

4.3.2 Transfer from syringe into measurement cell

The Swagelok SS-QM2-B-1PM Mini Connector mounted on the syringe creates a dead volume which affects the specific transfer efficiency from syringe to measurement cell. Thus, the specific transfer efficiency and its uncertainty have been quantified by experiment. They are then taken into account in the calculation of the total transfer efficiency from sample gas bottle to measurement cell.

Table 4.6: The experimental determination of residual sample gas within the gas-tight syringe.

Test Number	Xe Area before transfer	Xe Area after transfer	Residual factor [%]
1	1062332	37018	3.48
2	1068613	35520	3.3
3	1071946	35569	3.31
4	1085513	36953	3.42
5	1096370	37072	3.37

In a series of transfers from the syringe into the measurement cell, the specific transfer efficiency has been determined by experiment. Therefore, the amount of residual gas in the syringe after a transfer has been analyzed. As a first step, the syringe has been filled with roughly 10 cm^3 of a reference gas containing 30% Xe and 70% N_2. To determine the exact amount of gas in the syringe its xenon content is measured at the XMS. After a transfer into a previously evacuated measurement cell, the residual gas within the syringe

is analyzed again. Comparing the xenon content in both measurements allows to calculate the residual factor. The residual factor represents the ratio of the syringe's dead volume to the total volume of measurement cell and syringe. The average residual factor and its uncertainty amount to $(3.4 \pm 0.1)\%$.

4.3.3 Radioxenon measurement cells

There are five Measurement Cells (MCs) in use: MC1 to MC5. All measurement cells have been tested for leak tightness by three different methods.

1. Slight overpressure of helium in the cell and probing of the cell with a helium sensitive leak detector

2. Under-pressure in the cell and monitoring of the gas pressure for 24 hours

3. Activity measurement of the ^{133}Xe spiked cell over several days

Due to their construction design, the measurement cells of the third generation are sensitive against overpressure. Pressures exceeding 1.5 *bar* can destroy a measurement cell by pushing out the carbon window. It is therefore strongly recommended to always keep the pressure below 1.1 *bar* absolute pressure.

The memory effect of the design has been determined by using the same spike of the cross-contamination test. Because of the short half-life of ^{135}Xe, only ^{131m}Xe and ^{133}Xe have been used for testing the memory effect. A total decay corrected activity of 331 *Bq* has been transferred into the measurement cell. After exactly three days, the cell has been evacuated and analyzed again for residual activity. The total residual activity has then been determined to be 0.08 *Bq*.

Table 4.7: Results of the memory effect test.

Measurement	Stable Xe [cm3]	^{131m}Xe [Bq]	^{133}Xe [Bq]	Total [Bq]
Spike Sample	0.656	136	195	331
Residual	n/a	0.037	0.041	0.078
Memory effect [%]:	n/a	0.027	0.021	0.024

The total uncertainties to residual activity values have been 13% for ^{131m}Xe and 11% for ^{133}Xe.

By a factor of 10, the memory effect is clearly below the requirement of 0.3%. This result is based on an exposure time of three days and the presence of $(0.656 \pm 4\%)$ cm^3 stable xenon. For shorter exposure times and/or higher amounts of stable xenon, the memory effect is expected to be even smaller. The measurement cell has a Swagelok SS-QM2-B-1PM Mini Connector, through which it is filled and evacuated. The volume of the connector is $0.08cm^3$, which is less than 0.6% of the total volume (14.1 cm^3). The effects on the geometry of the radioxenon analysis have therefore been neglected.

4.3.4 Total transfer efficiency

The total transfer efficiency contains the bottle to syringe and the syringe to measurement cell specific transfer efficiencies. The transfer efficiency of the XTS depends on the sample composition and the volume of the archive bottle container. During a series of 20 transfers from SPALAX and SAUNA archive bottles into the measurement cells, the transfer efficiencies were found to be between 86% and 55%.

Based on these values, a minimal total transfer efficiency of about 55% can be seen as a minimum for routine samples. It therefore satisfies the technical requirement of 50% (CTBTO, 2012). However, in cases of samples including high amounts of nitrogen and/or moisture, the transfer efficiency will naturally deteriorate. This can be the case when an archive bottle is not completely air tight or when a sampling station has problems in the sample purification.

4.4 Calibration and validation of the radioxenon detection system

4.4.1 Calibration of the peak efficiency

The basis of the peak efficiency calibration of the radioxenon measurement geometry for both detectors Det3 and Det4 is the Canberra LabSOCS Monte Carlo based software. The accuracy of the LabSOCS characterization provided by the manufacturer has been validated by comparison with other standard geometries like beaker and filter sample which had already been calibrated experimentally by using traceable point and area sources.

In general, LabSOCS is found to be accurate to within 4-5% for energies greater than 400 keV and 7-11% at one standard deviation for energies between 50 and 400 keV. LabSOCS is estimated to be accurate within 15% for energies less than 50 keV.

Experimental data has in a second step been used to optimize the simulated efficiency calibration function. The resulting calibrations for both detectors have been validated and refined by comparative measurement of several samples on each detector.

Detector Det3 has been characterized by Canberra for LabSOCS calibrations in 2009. Since then, continuous monitoring of detector parameters such as FWHM and efficiency have shown a slight aging of the detector. In order to compensate for decreasing peak efficiencies, it was decided to establish a semi-empirical efficiency function based on LabSOCS simulated data points and traceable reference sources.

The LabSOCS calibration of the radioxenon measurement cell has served as a basis for the final peak efficiency calibration. Since LabSOCS uses a point-in-time characterization of the detector, long-term fading of the detector efficiency is not accounted for. It is however known that HPGe detectors are prone to degeneration, affecting the thickness of a natural deadlayer. Due to the construction design of BEGe detectors, a change in dead-layer thickness will manifest itself in two effects.

1. Decreased peak efficiency for all energies, due to a decreased active detector volume.

2. Decreased peak efficiency for low energies, due to attenuation in the dead layer.
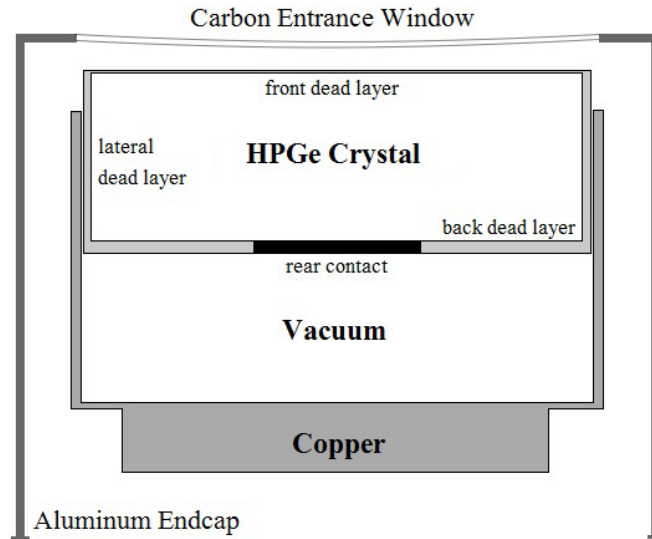
Figure 4.3: Schematic drawing of a detector crystal and possible dead layer zones

Together, both effects will yield slightly lower peak efficiencies, especially in the low energy region. Since the LabSOCS calibration itself does not take into account these effects, the efficiency function has been adjusted accordingly by harmonization with traceable standard point sources.

The final efficiency function of the third generation measurement cell geometry has been obtained through a compensated LabSOCS calibration. Using a set of six different point sources, it was found that LabSOCS in general overestimates the efficiency. Two point sources from Physikalisch-Technische Bundesanstalt (PTB) (^{133}Ba, ^{137}Cs) and five Amersham point sources (^{210}Pb, ^{241}Am, ^{133}Ba and ^{137}Cs) have been measured at different distances: 102 mm, 252 mm and 502 mm, with the exception of ^{133}Ba which, due to coincidence summing, has only been measured in 252 mm and 502 mm distance.

The stated total uncertainties include systematic and statistical contributions:

1. Uncertainties stated by the supplier: 0.55% for PTB and 1.5% for Amersham sources

2. Experimental variations of the two (in case of ^{133}Ba) or three different measurement

geometries

3. Counting statistics

Table 4.8: The results of the far distance measurements of eight different reference sources on Det3. The relative deviations are based on measured activity through Lab-SOCS efficiency calibration minus the traceable reference value.

Supplier	Nuclide	Energy [keV]	Deviation [%]	Tot Unc. (k=1) [%]
Amersham	^{210}Pb	46.5	-8.16	1.9
Amersham	^{241}Am	59.5	-4.51	2.0
Amersham	^{133}Ba	81	-3.70	1.7
PTB	^{133}Ba	81	-5.19	2.2
Amersham	^{152}Eu	122	-2.90	2.6
Amersham	^{152}Eu	244	-4.22	1.7
Amersham	^{152}Eu	344	-3.00	1.7
Amersham	^{133}Ba	356	-4.92	1.5
PTB	^{133}Ba	356	-4.04	0.7
Amersham	^{137}Cs	662	-3.08	1.9
PTB	^{137}Cs	662	-3.91	1.0

The deviation from the simulated efficiency was found to range from (-3%) to (-8%). While low energies show a stronger deviation, the deviation in the energy range from 80 keV to 662 keV lacks a significant trend. It is assumed, that either the uncertainty of the MCNP simulation itself or a possible dead layer on the detector crystal are the reasons for the deviation. However, the deviation is still well within the uncertainty stated by the supplier for LabSOCS calibrations.
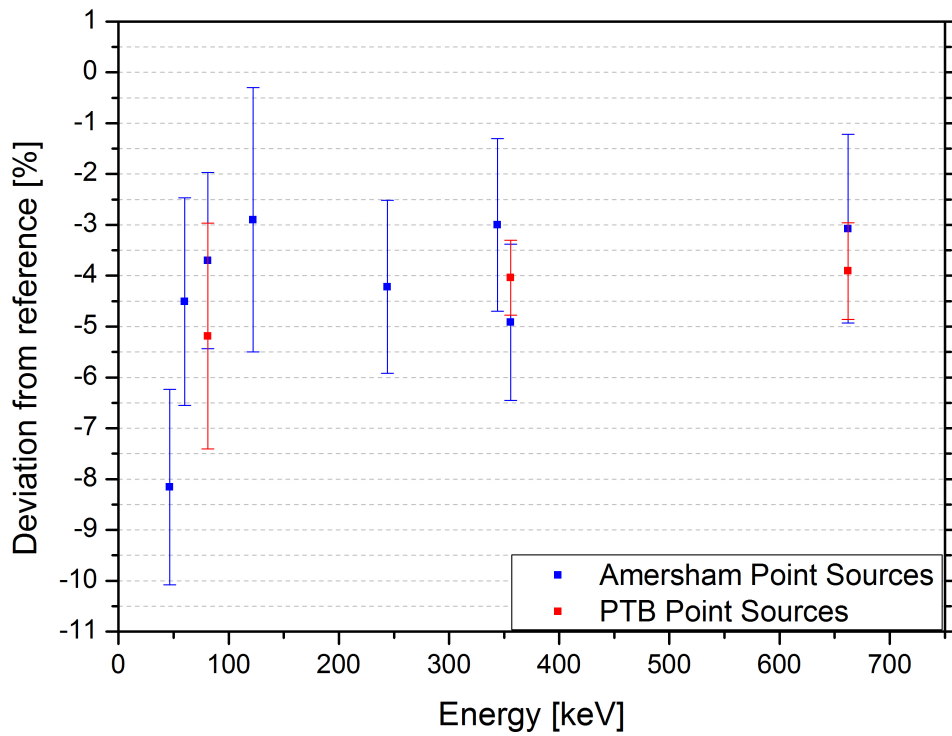
Figure 4.4: The deviations of measurement results from reference activities at different energies

As a corrective measure and to be able to generate a more precise efficiency function, the LabSOCS generated efficiency of the radioxenon measurement cell has been improved accordingly. A uniform scaling of (-4.5%) has been chosen as a compromise that fits the experimental data and is well within the uncertainty of the LabSOCS simulation.

Table 4.9: Detector efficiencies for the xenon measurement geometry for both detectors.

	Detector 3		Detector 4	
Energy [keV]	Efficiency [%]	Sigma [%]	Efficiency [%]	Sigma [%]
22.1	22.4	12	21.4	12
24.1	23.8	11	22.7	11
25.0	24.4	10	23.2	10
27.4	25.6	9	24.4	9
32.1	27.1	8	25.8	8
36.5	28.1	7	26.7	7
46.5	29.3	6	27.9	6
59.5	29.9	5.5	28.6	5.5
88.0	29.3	5	28.1	5
122.0	26.8	5	25.8	5
145.4	24.8	5	23.8	5
165.9	23.0	5	22.1	5
255.1	16.6	5	15.7	5
320.1	13.5	5	12.6	5

Detector Det4 has been characterized by Canberra for LabSOCS calibrations in 2014. Initial validation of the detector performance has been carried out, supporting all relevant detector parameters stated in the characterization report. Because of the very recent characterization, there are no reasons for aging effects, such as with Det3. Thus, Det4 efficiency calibration has been performed solely on the basis of the LabSOCS simulated data. 4.9 shows efficiency data points for the energy region of interest (30 keV - 250 keV).

4.4.2 Validation of detector efficiency calibration

A ^{133}Xe activity gas standard has been acquired and solely used for validation of the efficiency calibration. The ^{133}Xe activity and uncertainty ($k=2$) of the standard was 36.64($\pm$5.4%) kBq. By measuring the original sample container before and after a partial transfer into a previously evacuated measurement cell, the total activity within the measurement cell is well known. The validation of the efficiency function was two-fold:

1. Validation of the total ^{133}Xe activity in the measurement cell by using the 81 keV line.

2. Validation of the efficiency function at 30.9 *keV* by using well-known branching ratios (DDEP) (Galan, 2008).

For the measurement of the original sample container, a sample holder has been manufactured that keep the glass sphere in a reproducible geometry at a well-known distance to the detector. A 0.5 *mm* thick layer copper was chosen as an absorber to decrease the effect of x-rays and to reduce coincidence summing effects.

Part of the standard was then introduced into a measurement cell. The transfer factor was calculated by comparison of the count rate of the original standard before and after the transfer. It was found to be 27.8% which equals to 10.17 *kBq*.

The measured activity within the measurement cell was found to be 10.31 ($\pm$7.3%) *kBq* using the 30.9 *keV* line and 10.11 ($\pm$5.2%) *kBq* using the 81 *keV* line. The uncertainty of measurement comes to a large degree from the systematic uncertainty of the efficiency calibration. The analysis of both lines is in excellent agreement with the reference activity and well within its uncertainty.

Table 4.10: The results of the validation of measurement cell efficiency calibration for 30.9 *keV* and 81 *keV*.

E [keV]	Net counts	Branching Ratio [%]	Calibrated Efficiency [%]	Measured/True Activity	Theoretical Efficiency [%]
30.9	106366	38.5	26.25	1.01	26.61
81	111423	37.3	29.45	0.99	29.28

Taking into account the branching ratios of 38.5% (30.9 *keV*) and 37.3% (81 *keV*), theoretical efficiencies can be calculated to be 26.61% respectively 29.28%. The observed discrepancy is well within the uncertainty of the efficiency calibration. The measurement cell geometry has thus been successfully validated.

4.4.3 Validation through intercomparison exercises

The AXeL system has taken part in several intercomparison exercises. The CTBTO has launched a program of intercomparisons based on voluntary participation to stimulate

progress in the area of radioxenon analysis. Results showed biases in the results of the activity concentrations of 20 - 30% between the laboratories (Gohla et al., 2011; Gohla and Auer, 2013). Until 2014 intercomparison exercises lacked reference values, so that they only provided a means of comparison between laboratories rather than evaluation against a reference. However, the two last exercises conducted in April, 2014 and March, 2015 involved gas samples with reference values. The latter of which is still under evaluation and therefore not discussed in this work.

In 2014, a total of four activity concentration standards have been analyzed with AXeL. Two of which have been supplied by the Idaho National Laboratory (INL), the remaining two have been produced at Seibersdorf from ^{133}Xe activity standards traceable to NIST and obtained from Eckert & Ziegler. All four standards have been analyzed using the newly developed measurement cells and the semi-empiric efficiency calibration that has been described above.

Table 4.11: The results of ATL03 compared to reference values provided by INL.

INL	STP-Xe vol. $[cm^3]$	Uncertainty $(k=1)$ [%]	Act. Conc. ^{133}Xe $[mBq/m^3]$	Uncertainty $(k=1)$ [%]	Deviation from ref. [%]
Reference	1.10	1.8	168.8	1.55	-
ATL03	1.05	3.8	173.9	6.5	3.0
ATL03	1.08	3.7	167.9	6.4	-0.6

Figure 4.5: The results of the 2014 intercomparison exercise compared to the reference value provided by the Idaho National Laboratory (INL) and other participating laboratories.

The results of the intercomparison samples analyzed with AXeL show very good agreement to all four activity concentration reference gases. In each case, the reference value is well within one sigma of the combined uncertainty of the reference value and measurement result. On that basis, the performance AXeL system as a whole has been validated.

Table 4.12: The results of ATL03 compared to the reference values of the two in-house produced reference gases based on activity standards traceable to NIST.

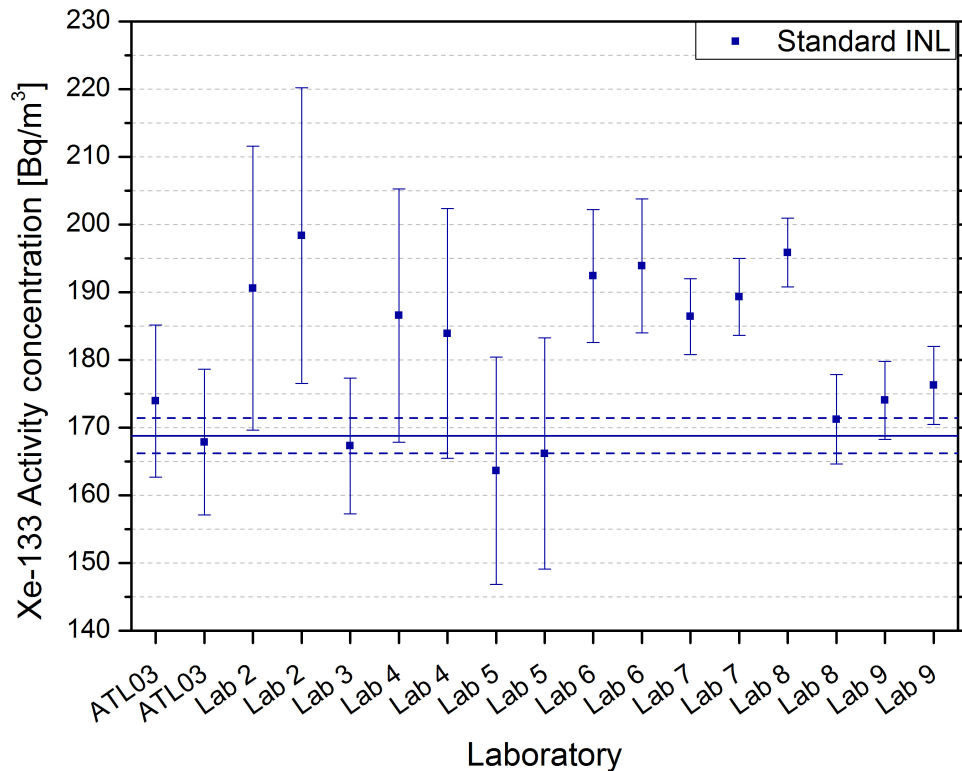| Seib. Lab.	STP-Xe vol. $[cm^3]$	Uncertainty $(k=1)$ [%]	Act. Conc. ^{133}Xe $[mBq/m^3]$	Uncertainty $(k=1)$ [%]	Deviation from ref. [%]
95853 Ref.	-	-	177.0	2.1	-
ATL03	1.05	3.8	172.4	6.4	-2.6
95854 Ref.	-	-	86.6	2.1	-
ATL03	0.97	4.1	83.9	6.9	-3.1
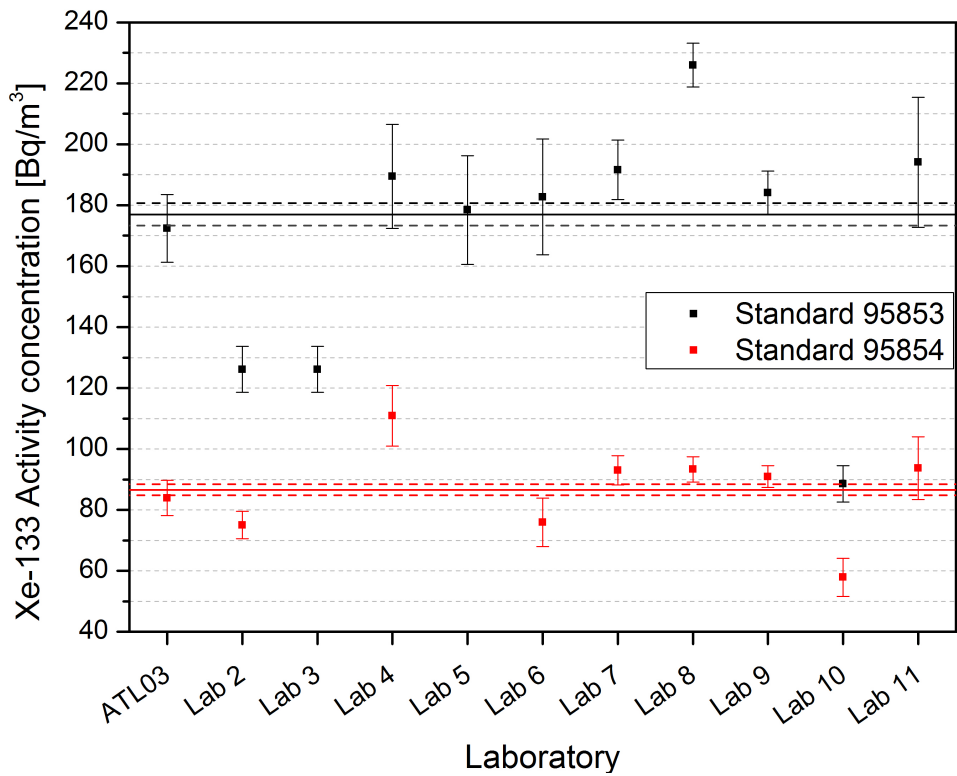
Figure 4.6: The results of the 2014 intercomparison exercise compared to the reference value provided by the ATL03. All uncertainties are given at $k=1$.

> All science is either physics
> or stamp collecting.
>
> *Ernest Rutherford*

5 Production of radioxenon isotopes

5.1 Introduction

The use of radioxenon isotopes is essential in testing and validation of any radioxenon analysis system. The main isotopes of interest are ^{131m}Xe, ^{133m}Xe, ^{133}Xe and ^{135}Xe. The gaseous radiation sources are called (radioxenon) spikes. Production of radioxenon spikes has been objective to several research projects in the past. The historically most established method is neutron irradiation of uranium targets and subsequent separation from other fission products. In radiopharmaceutical facilities this method yields radioxenon as a byproduct. The two most prevalent isotopes produced in this process are: ^{133}Xe and ^{135}Xe. But, because of the short half-life of ^{135}Xe, typically ^{133}Xe is the only radioxenon isotope that is commercially available. Since it is a nuclide commonly used in diagnostics, commercial providers offer ^{133}Xe as a radiopharmaceutical product. Typical activities are 37 GBq or higher with impurities of ^{131m}Xe, usually provided in glass vials, for example ^{133}Xe Draximage® vials of Draxis, Quebec, Canada.

Isotopic pure ^{133m}Xe spikes have been produced by the use of a Penning trap purification process. The isotopes have been produced by proton induced fission reaction of natural uranium. The recoiling isotopes have been thermalized by helium gas, and separated by their mass-over charge ratio. After further purification in a gas-free Penning trap, the isotopes have been implanted into a thin aluminium foil (Peräjärvi et al., 2008).

Recently, neutron irradiation of previously enriched xenon isotopes has been demon-

strated to be useful for the production of radioxenon isotopes (Haas et al., 2009). Enriched ^{130}Xe has been activated by neutron irradiation to ^{131m}Xe; ^{132}Xe to ^{133}Xe and ^{133m}Xe; and ^{134}Xe to ^{135}Xe. The resulting radioxenon isotopes have been analyzed by an ARSA-type beta-gamma system. ^{131m}Xe and ^{135}Xe spikes had purities of 99%. The method further achieves an isotopic ratio of 0.31 for ^{133m}Xe/^{133}Xe, which is significantly higher than from irradiation of uranium targets.

At ATL03, time constraints during testing of the AXeL system and the relatively short radioxenon half-lives led to the development of in-house radioxenon production capabilities. The aim was to establish radioxenon production methods able to generate readily available radioxenon isotopes in adequate activity and purity. Two methods of radioxenon isotope production have been developed for this purpose:

1. Production of ^{131m}Xe by decay from ^{131}I

2. Production of fission-type radioxenon mixtures by spontaneous fission of ^{252}Cf

Furthermore, commercially available ^{133}Xe activity standards have been acquired and used for the production of activity concentration standards, by the addition of traceable amounts of stable xenon. The dilution makes typical activity standards useable for AXeL and other highly sensitive measurement systems. They proved as a valuable tool for the calibration of a detector set-up and for intercomparison exercises.

Radioxenon spikes are produced in a C-type laboratory for handling radioactive material. As the spikes are being applied to highly sensitive measurement systems effective removal of contaminants is mandatory. Moreover, since the production of radioxenon involves high activities of ^{131m}I and ^{252}Cf, radiation safety plays an important role. For bleeding off the generators and handling of the spikes 50 cm^3 and 20 cm^3 gas tight syringes are used (Vici). They are equipped with a valve and a Swagelok miniconnector. The Quality Assurance Program for the production of radioxenon isotopes involves a strict separation of "dirty" and "clean" syringes. Every syringe used for spike production is either marked dirty or clean. Dirty syringes have female mini connectors. They are used for bleeding off the generators and are therefore contaminated and have to stay in the C-Lab. Through a purification step, radioxenon spikes are transferred into clean sy-

ringes. Clean syringes have male mini connectors and may be used in and outside the C-Lab. Whenever a clean syringe is brought into the C-Lab, it needs to be prepared as to minimize the risk of outside contamination. This is achieved, by placing the previously evacuated clean syringe into a plastic bag. Only the mini connector pierces the plastic bag.

5.2 Generation of radioxenon isotopical mixtures using ^{252}Cf

5.2.1 Californium-252

Californium was first synthesized in February 1950 through alpha bombardment of ^{242}Cm. These experiments took place at the radiation laboratory in Berkeley of the University of California, the state which the element was named after. There are 18 known isotopes of californium from ^{237}Cf to ^{256}Cf. Most californium isotopes decay through alpha emission; some show a spontaneous fission decay branch.

Californium is produced through neutron capture of transuranic elements in nuclear reactors. It is mainly comprised of ^{252}Cf, which is also the isotope most commonly used in industry, medicine and research. Since the mid-1960s, weighable amounts of ^{252}Cf are typically being obtained in high flux nuclear reactors, such as the High Flux Isotope Reactor at Oak Ridge National Laboratory.

Cf-252 primarily decays through alpha emission. The half-live of 2.6 years and the 3.09% decay branch of spontaneous fission however make ^{252}Cf a convenient neutron emitter. With a multiplicity of 3.8 neutrons per fission and an 85 year half-life in respect to spontaneous fission, the calculated emission rate is $2.3 * 10^{12}$ neutrons $s^{-1}g^{-1}$ (Be and Chiste, 2008). There are numerous publications including biological studies and dosimetry, radiotherapy, neutron radiography and neutron activation analyses. Spontaneous fission of ^{252}Cf produces high energy neutrons, with an energy spectrum which is very similar to induced or spontaneous fission of uranium isotopes. The majority of its applications in

industry and research make use of ^{252}Cf as a neutron emitter (Yevgeni A. Karelin et al., 1997). Because of its spontaneous fission decay branch it has also found application as a source of fission fragments (Duellmann et al., 2003).

In general, there are two types of ^{252}Cf sources commonly in use. Typical ^{252}Cf neutron sources have the form of a doubly encapsulated, welded container that prevents leakage of fission products. Fission foil sources of ^{252}Cf however are unsealed sources. They usually are available in activities up to a few MBq and are used for fission fragment spectrometry. Since they are unsealed, this type of source constantly emits fission fragments. The spectrum and yield of fission fragments is slightly different compared to the neutron spectra and fission yields of ^{235}U or ^{239}Pu. Atomic californium, like all actinides, is very reactive especially with water vapor, oxygen and acids (Baybarz et al., 1972). Therefore, chemically stable californium(III)-oxide (Cf$_2$O$_3$) is usually being used for ^{252}Cf sources (Balo et al., 1999; Wiltshire, 1985).

5.2.2 Design of the AXG1

With the aim to generate and obtain radioxenon isotopes, a 1.85 MBq ^{252}Cf fission foil source has been acquired from Amersham. The fission foil source consists of a 12.7 mm diameter and 0.127 mm thick platinum-cladded nickel foil. The active area is a 5.04 mm diameter spot of electrodeposited californium(III)-oxide (Cf$_2$O$_3$) centered in the middle of the nickel foil.

During fission most of the energy is given to the fission fragments, which in a second step can collide with ^{252}Cf nuclides. In thin films this results in kick-out of ^{252}Cf atoms. This phenomenon makes ^{252}Cf volatile. To prevent loss of ^{252}Cf by kick-out, the active area is covered by a 50 $\mu g/cm^2$ layer of gold. Because of its high weight density and atomic number, gold is an excellent absorber for particle radiation and especially heavy ions. While the gold layer retains ^{252}Cf, it is thin enough to allow most fission fragments to pass.

A specially designed gas tight aluminium container has been built to house the ^{252}Cf

source. The Austrian Xenon Generator 1 (AXG1) has a total volume of (10 ± 0.2) ml, which is filled with a carrier gas to decelerate the fission products, and a male Swagelok Mini Connector to fill and elute the volume. The container normally contains pure nitrogen gas (N_2). The pressure of nitrogen gas in the generator has to be maintained above a critical level of 2 bar. This is necessary to ensure efficient deceleration of the fission products, to keep the yield of the generator high. The maximum range of fission products in air at atmospheric pressure is about 22 mm. The generator offers a path for deceleration of about 13 mm. This results in a pressure limit of 1.7 bar for pure nitrogen.

Figure 5.1: Left: The ^{252}Cf foil in its original container. Middle: The AXG1 aluminium container with the connector valve. Right: The ^{252}Cf foil glued onto the cap of the AXG1.

For storage, a safety tip is placed onto the Swagelok Mini Connector valve to prevent accidental release from the AXG1. It is further kept in a gas-tight, evacuated and sealed plastic foil. Failure of the gas-tightness of the aluminium container will therefore be visible to the user prior to opening the plastic foil. The plastic foil is to be replaced after each application of the generator. The generator is stored within a neutron shielding, that mainly consists of two blocks of borated parrafin. Each block has a length and width of 21 cm and a height of 10 cm. A storage volume has been cut out the lower block for the AXG1. Both blocks fit into a casing that is covered on the inside by 2 mm thick cadmium sheets.

5.2.3 Performance of the AXG1

The generator AXG1 holds a $(1.85 \pm 0.15) \, MBq$ source of ^{252}Cf (as of November 15, 2011). Fission fragments that are directed into the platinum cladded nickel foil are implanted into the foil and cannot be emanated. Based on the geometry of the container, that gives a theoretical yield of almost 50%. As already mentioned above the production of radioxenon spikes involves a strict separation of "dirty" and "clean" syringes. The AXG1 generator is eluted by connecting a dirty syringe (marked "^{252}Cf only") and drawing off gas by pulling the plunger. The syringe volume will define the total activity of the spike. The gas is split into the volume of the generator ($10 \, ml$) and the volume of the syringe ($50 \, ml$) resulting in an extraction efficiency of up to 80%. For weak spikes a syringe volume of a few cm^3 will be enough, while maximum activity elution is achieved by pulling the plunger to the maximum syringe volume. The typical total emanation yield for radioxenon isotopes lies between 30 and 40%.

The syringe now contains fission products and even traces of ^{252}Cf. Therefore, the eluent needs to be filtered. The filter is $14 \, cm$ long 1/8 inch steel tube filled with 50x80 mesh sized silver exchanged mordenite AgZ. Mordenites form a class of natural and synthetic zeolites that show high chemical stability. Once the syringe valves are opened, gas will flow through the zeolite filter into the evacuated clean syringe. By pushing the plunger of the dirty syringe carefully, the total amount of eluent gas is transferred into the filter tube and further into the clean syringe.

Figure 5.2: The filter tube used for separation of particulate and aerosol-bound fission products from noble gases.

Once the transfer is completed, the syringes are closed and disconnected. The AXG1 needs to be filled again with nitrogen carrier gas to $2 \, bar$ absolute pressure. It is placed back into its shielding for further use. The clean syringe is unwrapped carefully from its

plastic bag without contaminating the syringe itself. It is then brought out of the C-Lab for gamma spectroscopic analysis in an especially designed syringe holder.

The activity of the final spike or spikes can then be altered by the use of other syringes and manifolds. If needed, the spike is diluted by connecting the syringe to other syringes filled with carrier gas and splitting the spike volumetrically. The radioxenon activities within the syringes will be proportional to their respective volumes.

Particulate radionuclide fission products are effectively separated by the zeolite filter. Noble gas fission products however pass the zeolite filter. A mix of all four radioxenon isotopes but mainly ^{133m}Xe, ^{133}Xe and ^{135}Xe can be obtained from the AXG1 (see 5.3). The maximum activities that can be withdrawn from the generator are about 40% of its total content. They amount to 20 Bq ^{133m}Xe, 680 Bq ^{133}Xe and 820 Bq of ^{135}Xe.
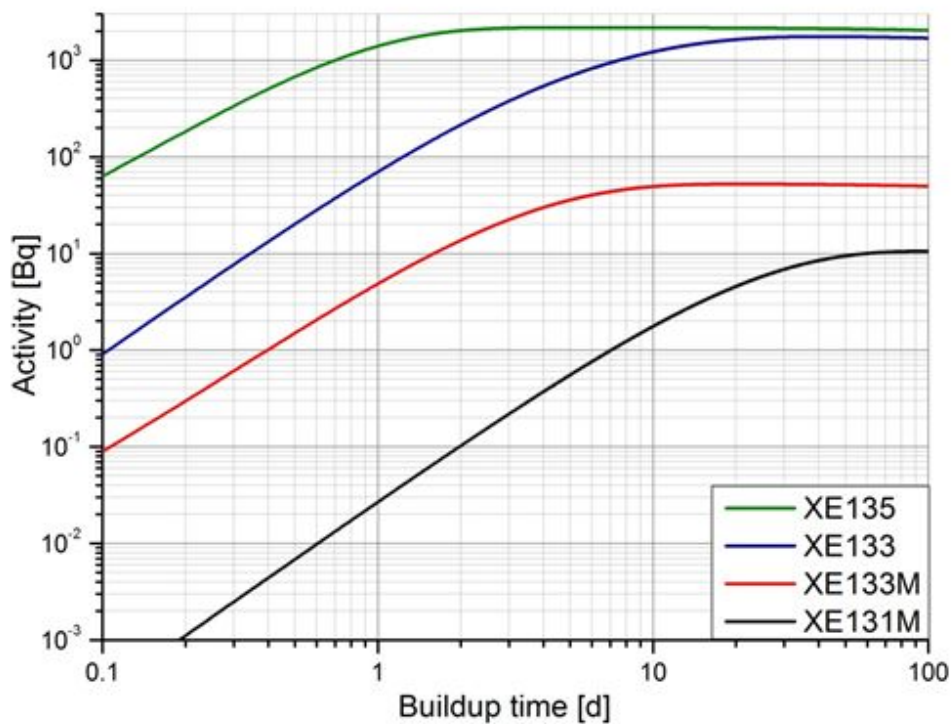
Figure 5.3: The total build-up of radioxenon within the AXG1 generator over time.

Depending on the build-up and decay time, the AXG1 will give different isotopic signatures. Xe-131m has the smallest fission yield and considerable activities are therefore

only present in mixtures with the three other radioxenon isotopes. The production of pure ^{131m}Xe is covered by the Austrian Xenon Generator 2 (AXG2) (see section 5.3). Xe-133m can be produced as part of a mixture with ^{133}Xe and ^{135}Xe. The ratios of ^{135}Xe/^{133}Xe and ^{133m}Xe/^{133}Xe can be chosen to some degree depending on the buid-up time (see 5.4). Xe-133 can be drawn off to maximum activities of 680 Bq in a mixture with ^{135}Xe. After a decay time of 3 days, ^{133}Xe activity will be 450 Bq, with other radioxenon isotopes present at less than 5 Bq. Xe-135 is the radioxenon isotope with the highest fission yield and the shortest half-live. In any fresh AXG1 spike ^{135}Xe is the prevalent isotope in terms of activity. After a build-up time of 3 hours, a spike will contain 30 Bq of ^{135}Xe, with less than 1 Bq of other radioxenon isotopes.
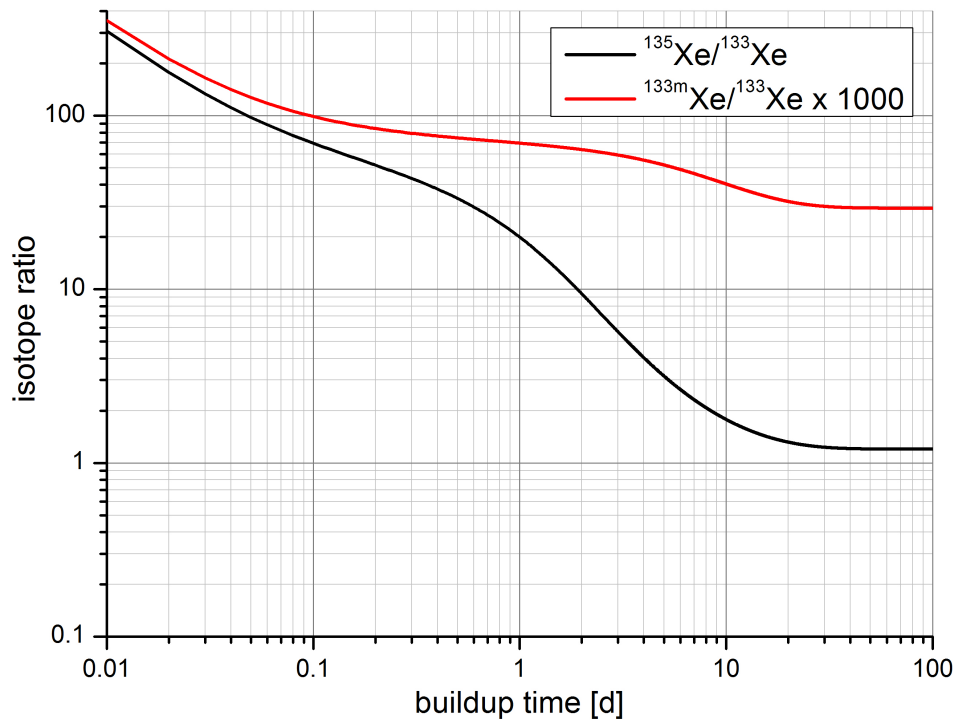
Figure 5.4: The ratios of the drawn-off activities of ^{135}Xe/^{133}Xe and ^{133m}Xe/^{133}Xe over time.

The AXG1 design can therefore be utilized for the production of ^{133}Xe and ^{135}Xe spikes that have very little activities of other radioxenon isotopes. The metastable isotopes ^{131m}Xe and ^{133m}Xe can be obtained in mixtures with ^{133}Xe and ^{135}Xe. By choosing build-

up and decay times the AXG1 can further deliver radioxenon mixtures of many different isotopic signatures.

5.3 Generation of ^{131m}Xe using ^{131}I

5.3.1 Radioiodine ^{131}I

For the production of ^{131m}Xe the radioisotope ^{131}I has been chosen. I-131 disintegrates through beta minus decay into the stable ^{131}Xe and its isomeric state ^{131m}Xe at 163.93 keV. It has an half-life of 8.0233(19) d and a branching ratio of 0.48% into ^{131m}Xe (Chiste and Be, 2014). With a cumulative fission yield of 2.9% for thermal fission of ^{235}U, ^{131}I is a major radionuclide produced in nuclear fission (England and Rider, 1994). I-131 is being used widely in medicine for treatment as well as in imaging methods and thus commercially available from several suppliers.

Because of its high volatility and its role in human metabolism, radioiodine poses a considerable risk to human and ecological health (Ethan M. Cox and Yuji Arai, 2014). In terms of applicability, radioiodine needs to be separated from radioxenon to prevent impurities in the eluent and contamination of radioxenon detection systems. Because of these aspects the AXG2 has to offer a highly effective containment of radioiodine. Design and handling of the AXG2 generators reflect the necessity to prevent loss of radioiodine from the generator into the environment.
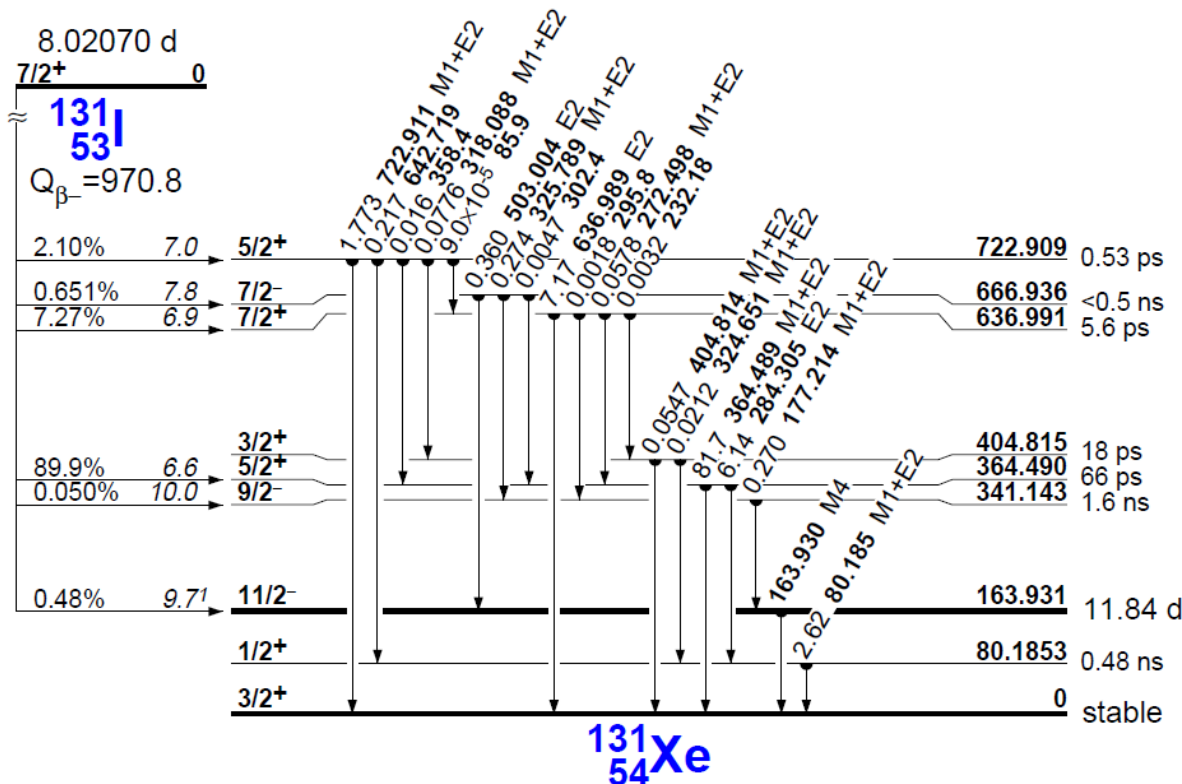
Figure 5.5: Decay scheme of I-131 (Firestone, 1999)

Highly concentrated (>500 mCi/mL) ^{131}I in 0.1 M NaOH has been acquired from PerkinElmer Inc., USA, to serve as the feed material. The alkaline solution has a pH of 10-12 (PerkinElmer, 2010). Total iodine solubility strongly depends on the pH of the solution (Kahn and Kleinberg, 1977; Clément et al., 2007). In acidic and neutral solutions iodide (I^-) oxidizes with time into elemental iodine (I_2) and iodates (IO_3^-). In contrast to iodide, elemental iodine has only a slight solubility in water with 1 g dissolving in 3450 g water at 20 $°C$ (Windholz et al., 1976). Highly alkaline solutions, however, are reported to maintain the iodine in the form of iodide and therefore soluble. They also show good stability against the exposure to gamma rays (Kahn and Kleinberg, 1977).

5.3.2 Design and loading of the AXG2

The ^{131m}Xe Generator consists of a steel tubing of 1/4 inch outer diameter and a thickness of 1.2 mm. With a total length of 145 mm the tubing is closed by a steel nut on one

side, on the other end it has a male Swagelok Mini Connector valve. The generator has a volume of about 3 cm^3, which is filled with nitrogen. The male Swagelok Mini Connector valve allows eluting and refilling the generator. It automatically closes when disconnected. For storage a safety tip is placed onto the Swagelok Mini Connector valve to prevent accidental release.

Figure 5.6: The AXG2 work desk: two open generators with two Petrianov filter sheets, the silver nitrate solution and the lead shieldings for transport.

Silver is known for its affinity for iodine and therefore it has been incorporated in various forms as a solid adsorbent for iodine removal (Haefner and Tranter, 2007). This includes silver exchanged zeolites and silver impregnated substrates. Both will find application in the iodine removal process of the AXG2. In all cases, the main reaction product is silver iodide AgI. AgI is stable at room temperatures but, like all silver halides, sensitive against exposure to light.

As a first step, 3 x 3 cm sheets of cellulose Petrianov filter FPP-15-1.5 material are wetted with a solution of 5 g silver nitrate $AgNO_3$, 5 g Isopropyl alcohol C_3H_8O and 40 g deionized water. Silver nitrate is commonly used to precipitate iodide I^- as silver iodide AgI. Silver nitrate impregnated substrates have also been demonstrated to successfully bind and remove elemental iodine I_2 (Haefner and Tranter, 2007; Clément et al., 2007). Once a filter sheet has been applied with the radioiodine solution, it is placed into the generator tubing and thus screened from light. Because of the relatively short half-life of eight days, the generator has to be reloaded on a regular basis, depending on the planned activity of the spikes. Each AXG2 is loaded with approximately 37 MBq (1 mCi) of ^{131}I. Approximately 0.2 μL of the radioiodine solution are applied to one filter sheet. After the solution has completely been absorbed by the filter paper, it is carefully folded and twisted in a way to keep the point of iodine application inside. The now cylindrical filter sheet is then placed inside the open generator tubing. The generator is carefully closed and checked for outside contamination. It is then evacuated and filled with nitrogen to about 1 bar, which serves as a carrier gas. Both generators are then transferred into the lead shielding for radioxenon buildup.

5.3.3 Performance of the AXG2

Because of the low branching ratio, it is necessary to charge the generator with a relatively large activity of ^{131}I. The initial activity of 1 mCi (37 GBq) of ^{131}I has been chosen as a compromise between ^{131m}Xe yield and the handling. The maximum ^{131m}Xe activity of one generator then amounts to about 100 kBq. As already described above the production of radioxenon spikes involves a strict separation of "dirty" and "clean" syringes. The AXG2 generators are eluted by connecting a dirty syringe and drawing off gas by pulling the plunger. The syringe volume will define the total activity of the spike. The gas is split into the volume of the generator (3 ml) and the volume of the syringe (1-20 mL) resulting in an extraction efficiency of up to 80%. For weak spikes a syringe volume of a few cm^3 will be enough, while maximum activity elution is achieved by pulling the plunger to the maximum syringe volume.
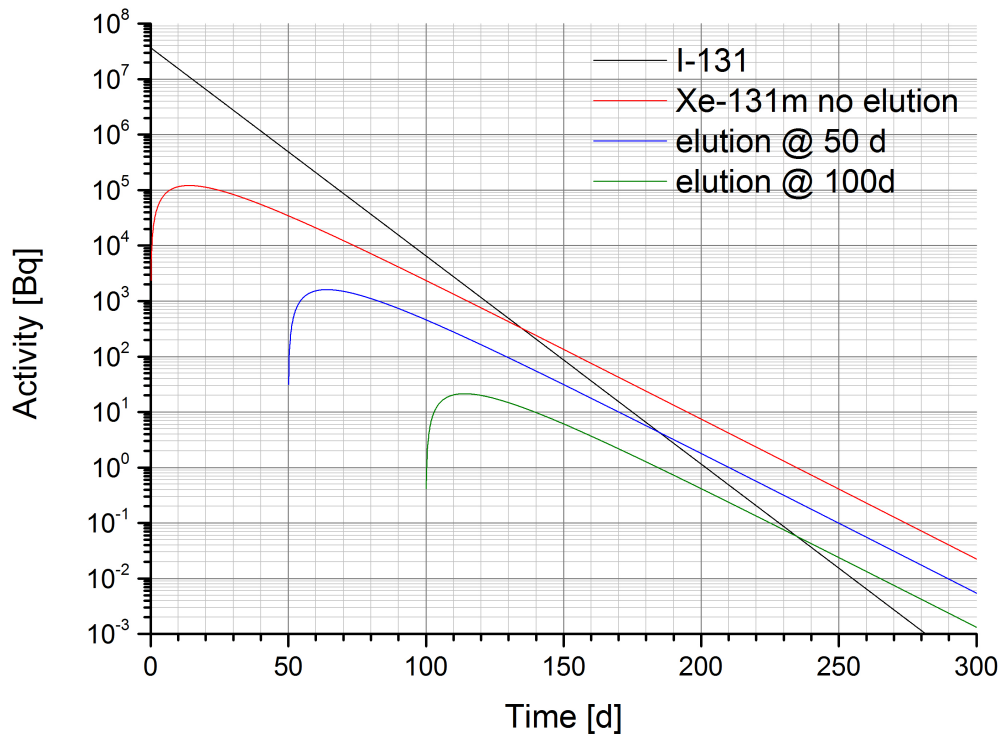
Figure 5.7: Ingrowth and decay of ^{131m}Xe for different elution times.

The eluent now contains measurable amounts of ^{131}I (up to several hundred kBq) which have to be separated from the ^{131m}Xe. Therefore, in a second step a filter tube is connected to both, the dirty and the clean syringe. The filter is 22 cm long 1/8 inch steel tube filled with 50x80 mesh sized silver exchanged mordenite AgZ. Mordenites form a class of natural and synthetic zeolites that show high chemical stability. The porous structure, its filtering qualities and high surface area make it an excellent adsorbent for iodine capture (Kepak, 1990; Haefner and Tranter, 2007). Once the syringe valves are opened, gas will flow through the zeolite filter into the evacuated clean syringe. By pushing the plunger of the dirty syringe carefully, the total amount of eluent gas is transferred into the filter tube and further into the clean syringe.

Once the transfer is complete, the syringes are closed and disconnected. The AXG2 is filled again with nitrogen carrier gas to 1 bar absolute pressure. It is placed back into its shielding for further use. The clean syringe is unwrapped carefully from its plastic bag

without contaminating the syringe itself. It is then brought out of the C type laboratory for gamma spectroscopic analysis in an especially designed syringe holder.

The activity of the final spike or spikes can then be altered by the use of other syringes and manifolds. If needed, the spike is diluted by connecting the syringe to other syringes filled with carrier gas and splitting the spike volumetrically. The radioxenon activities within the syringes will be proportional to their respective volumes.

The AXG2 design makes use of three retention mechanisms:

- The ^{131m}Xe is obtained in a solution of 1 M NaOH with a pH of 12-14. In highly alkaline solutions, iodine remains in the form of I$^-$ and thus soluble.

- AgNO$_3$ is used as a precipitator to form stable silver iodide AgI, when the radioiodine solution is applied to a filter sheet.

- A zeolite filter works as an adsorbent for remaining iodine in the eluent.

During two years of operation, around 50 ^{131m}Xe spikes with activities from 10 Bq to 100 kBq have been obtained from the AXG2 design. All ^{131m}Xe spikes have been analyzed on the Det3 system with suitable sample holders. Analysis showed that the AXG2 design successfully retained contaminations of ^{131}I. The decontamination factor of the AXG2 design has been determined after a 12 hour measurement of a ^{131m}Xe spike freshly loaded generator. The spike was found to be free of ^{131}I. The applicable MDA for ^{131}I of the measurement was 1.3 Bq. Thus, the decontamination factor based on the total ^{131}I activity is better than 1 : 10^9.

5.4 Production of activity concentration reference samples

Xenon-133 activity standards are commercially available from Eckert & Ziegler Isotope Products GmbH, Berlin, Germany. The gas standard consists of radioxenon and stable carrier gases at a pressure of about 0.85 bar. Its radioxenon isotopic signature is the same

or similar as ^{133}Xe for medical diagnostics, since it is being produced by irradiation of fissile material. Thus, besides ^{133}Xe the standards contain impurities of the longer-lived ^{131m}Xe. Eckert & Ziegler activity standards however provide reference activities for ^{133}Xe that are traceable to NIST.

The gas standards are contained in gas-tight, spherical vials of fused silica glass. They typically contain a gas volume of about 33 cm^3. The glass spheres have two connection arms, each equipped with a cone valve. The cone valves are greased to ensure gas-tightness.

Figure 5.8: Four ^{133}Xe standards as they are supplied by Eckert & Ziegler / Analytics.

A total of seven ^{133}Xe gas standards have been acquired in two batches. Of the seven standards, two have been used for direct validation of the efficiency calibration of the detector systems Det3 and Det4. The remaining five standards have been processed to serve as activity concentration standards by adding traceable amounts of stable xenon.

As a first step, the gas-tightness of the original container, i.e. the glass vials, is validated by gamma spectrometry. Each vial is repeatedly measured in a reproducible geometry at a well-known distance to the detector. A 0.5 mm thick layer copper has been chosen as an absorber to decrease the effect of x-rays and to reduce coincidence summing

effects. Over a time period of at least seven days loss of activity has not been observed. Statistical fluctuations have been less than 0.5%.

Figure 5.9: A ^{133}Xe standard with a connector valve mounted on detector Det3.

One connection arm of the glass vial has then been connected to a male Swagelok Mini Connector valve. Teflon compression rings ensure gas-tightness between the glass metal connection. The standard has then been transferred into a container, suitable to hold large amounts of additional xenon. Therefore, a previously evacuated Linde Minican (1 liter aluminium can) has been connected to the glass vial. Opening the connecting valves lets most of the gas content flow into the Minican. Pressurized air flushes remaining gas in the glass sphere in pulses. The glass containers are analyzed for residual activity after the transfer. In each case, the activity remaining in the glass container was less than 0.01% of the total activity. The residual activity is found mainly within the grease of the two cone valves. The loss of activity due to residuals can be neglected.

After the transfer, the Minican is disconnected. A well-known amount of stable xenon gas (>99.999% Xe) is added and the amount is quantified gravimetrically by the use of traceable balances. The exact gas composition of the EZ standards is not stated in the certificate. In the most adverse case of pure xenon at 0.85 bar, a total of about 28 cm^3 xenon (0.165 g) will add to the total xenon content in the activity concentration spike. This effect is taken into account as a systematic uncertainty in the uncertainty budget. It

is preferable therefore to add a large amount of stable xenon, typically 10 g to 30 g. The Minican then contains the total activity of the ^{133}Xe standard, a well-known amount of xenon and pressurized air, that has been used to ensure a complete transfer of activity. Thus it has a gas pressure of 5 to 8 bar.

To facilitate fast mixing, a method to induce eddy diffusion by thermal convection within the gas bottle is applied. The bottom of the Minican is heated to about $70°C$, while the top is cooled to $10°C$ for six hours. One standard has been used for validation of the uniform distribution of activity within the concentration standard. A series of samples has been taken from the full, half-full and almost empty gas bottle. The samples have been analyzed for their ^{133}Xe activity concentrations. Apart from statistical fluctuations of less than 1%, it has shown a uniformly mixed distribution of activity.
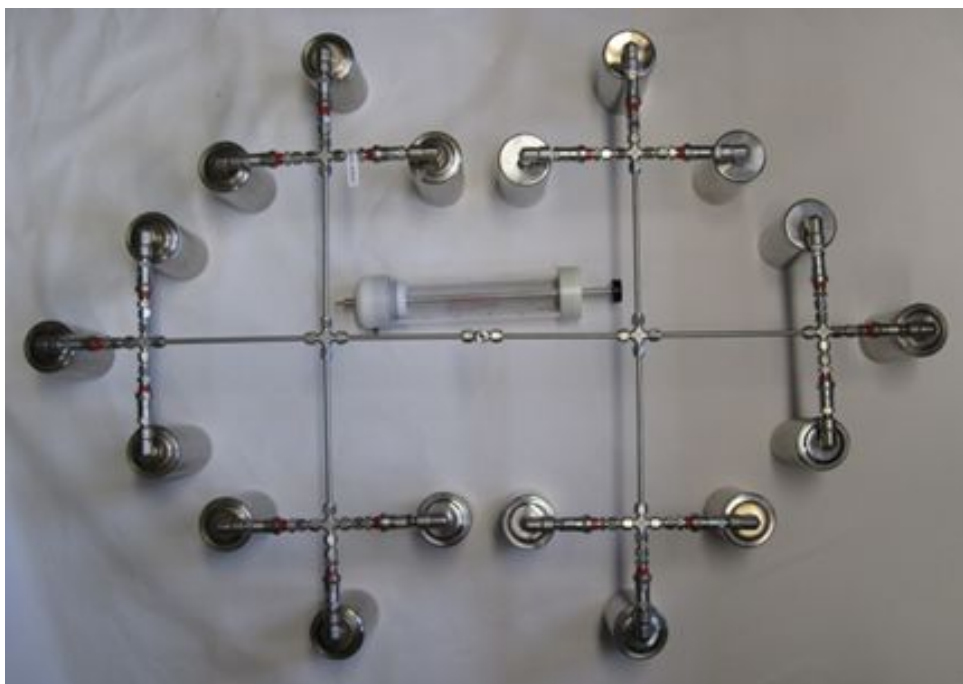
Figure 5.10: A manifold has been used for equal splitting into up to 18 gas bottles.

At the end of the production the Minican contains a well-known and traceable amount of stable xenon and a certified activity of ^{133}Xe. Using of a manifold, part of the activity concentration into archive bottles. The resulting activity concentration standard offers the opportunity to validate the AXeL system and other radioxenon analysis systems. During two intercomparison exercises in 2014 and 2015 this method has been applied to

produce reference samples. During these intercomparison exercises, a second producer of reference samples, the Idaho National Laboratory (INL), supplied additional reference samples (Gohla and Blanchard, 2015; Gohla et al., 2015).

> There is much pleasure to be gained
> from useless knowledge.
>
> *Bertrand Russell*

6 Conclusions

This work presents the successful continuation of research efforts in supporting CTBT verification regime at the Austrian radionuclide laboratory ATL03: the development and validation of AXeL (Austrian Xenon Laboratory), a laboratory system for radioxenon analysis.

AXeL consists of four automatic modules that can process and analyze atmospheric samples of all four radioxenon sampling systems within the IMS: ARIX, ARSA, SAUNA and SPALAX. A method for the injection of neon as an internal standard gas has been developed. As a first step in the analysis, the internal standard method allows accurate and reliable determination of stable xenon content. The measurement is performed by an automated gas chromatograph system, that compares the sample chromatogram to a reference gas with known neon and xenon content. The measurement is therefore independent of ambient conditions. The typical uncertainty of measurement is 4%.

To prepare the sample for gamma spectrometry, a method of sample transfer has been introduced which relies on a xenon trap based on activated charcoal. The sample is transferred into a gas-tight syringe and analyzed again for its stable xenon content. The total transfer efficiency has been found to be at least 55%. The effect of cross-contamination between subsequent samples has been determined to be as low as 0.2%.

Two ultra-low background HPGe detector systems have been built up in past research projects. AXeL utilizes these readily available detector systems for radioxenon quantification by gamma spectrometry. Gas-tight radioxenon measurement cells have

been designed and manufactured out of low-level copper and carbon windows coated with $2\ \mu m$ of aluminium in order to optimize detection efficiencies while keeping the memory effect below 0.3%. Within six days of acquisition the Minimum Detectable Activities for the four CTBT-relevant radioxenon isotopes ^{131m}Xe, ^{133m}Xe, ^{133}Xe and ^{135}Xe are found to be 1.3 mBq, 2.4 mBq, 1.8 mBq, and 4.9 mBq respectively.

AXeL therefore fully complies with the technical requirements of the CTBTO for radioxenon laboratories within the IMS. The accuracy and precision of the AXeL system have been validated thoroughly in experiments. Taking part in intercomparison exercises AXeL showed excellent agreement to the reference values. As a consequence, AXeL has become the first laboratory system to be certified by the CTBTO for atmospheric radioxenon analysis in December 2014.

The second part of this work concentrates on the methods for radioxenon production. During the development of AXeL, the need for radioxenon isotopes became imminent. Therefore, two radioxenon production methods have been developed: the Austrian Xenon Generators AXG1 and AXG2. The production methods are based on the radioactive spontaneous fission decay branch of ^{252}Cf respectively the radioactive decay of ^{131}I into ^{131m}Xe.

In addition to that, activity concentration reference gases have been produced based on commercially available secondary ^{133}Xe gas standards that are traceable to NIST. The method relies on the dilution of a traceable activity with large amounts of stable xenon. It has been applied to produce samples with well-known radioxenon content for intercomparison exercises.

Monitoring of radioxenon becomes more important within the IMS, especially after DPRK's recent nuclear weapons tests. Radioxenon as a verification tool has proven essential in identifying the explosion events to be of nuclear origin. Many IMS laboratories have therefore started to build up capabilities in radioxenon analysis. The certification of AXeL marks a significant milestone in the strengthening of the IMS network and represents a successful completion of work.

The importance of readily available radioxenon isotopes for system testing and vali-

dation should not stay unmentioned. The two methods presented herein allow the production of all four radioxenon isotopes of interest, a vital precondition for the development of AXeL. By being able to produce radioxenon isotopes, ATL03 also supports the CTBTO in the calibration and the quality control of radioxenon sampling stations. Thus, the work presented in this thesis is a valuable contribution to ongoing research efforts in the field of radioxenon analysis.

References

Auer, L., N. Rosenberg, K. Birdsell, and E. Whitney
    1996. The effects of barometric pumping on contaminant transport. *Journal of Contaminant Hydrology*, 24(2):145–166.

Auer, M., A. Axelsson, X. Blanchard, T. Bowyer, G. Brachet, I. Bulowski, Y. Dubasov, K. Elmgren, J. P. Fontaine, W. Harms, J. C. Hayes, T. R. Heimbigner, J. I. McIntyre, M. E. Panisko, Y. Popov, A. Ringbom, H. Sartorius, S. Schmid, J. Schulze, C. Schlosser, T. Taffary, W. Weiss, and B. Wernsperger
    2004. Intercomparison experiments of systems for the measurement of xenon radionuclides in the atmosphere. *Applied Radiation and Isotopes*, 60(6):863–877.

Auer, M., T. Kumberg, H. Sartorius, B. Wernsperger, and C. Schlosser
    2010. Ten years of development of equipment for measurement of atmospheric radioactive xenon for the verification of the CTBT. *Pure and Applied Geophysics*, 167(4-5):471–486.

Balo, P., J. Knauer, and R. Martin
    1999. *Production, Distribution, and Applications of Californium-252 Neutron Sources.*

Baybarz, R., R. Haire, and J. Fahey
    1972. On the californium oxide system. *Journal of Inorganic and Nuclear Chemistry*, 34(2):557 – 565.

Be, M. and V. Chiste
    2007-2008. Cf-252. *Decay Data Evaluation Project.*

Bjurman, B., L.-E. De Geer, I. Vintersved, A. Rudjord, F. Ugletveit, H. Aaltonen, K. Sinkko, A. Rantavaara, S. Nielsen, A. Aarkrog, and W. Kolb
    1990. The detection of radioactive material from a venting underground nuclear explosion. *Journal of Environmental Radioactivity*, 11(1):1–14.

Bowyer, T., K. Abel, W. Hensley, C. Hubbard, A. McKinnon, M. Panisko, R. Perkins, P. Reeder, R. Thompson, and R. Warner

1996. Automatic radioxenon analyzer for CTBT monitoring. *Automatic Radioxenon Analyzer for CTBT Monitoring.*

Carrigan, C. and Y. Sun

2014. Detection of Noble Gas Radionuclides from an Underground Nuclear Explosion During a CTBT On-Site Inspection. *Pure and Applied Geophysics*, 171(3-5):717–734.

Carrigan, C. R., R. Heinle, G. B. Hudson, J. J. Nitao, and Zucca J. J.

1996. Trace gas emissions on geological faults as indicators of underground nuclear testing. *Nature 382, 528 - 531.*

Chiste, V. and M. Be

2001-2014. Xe-131m. *Decay Data Evaluation Project.*

Clément, B., L. Cantrel, G. Ducros, F. Funke, L. Herranz, A. Rydl, G. Weber, and C. Wren

2007. State of the Art Report on Iodine Chemistry. *OECD NEA/CSNI/R(2007)1.*

Cronkite, E., R. Conard, and V. Bond

1997. Historical events associated with fallout from Bravo Shot- Operation Castle and 25 y of medical findings. *Health Physics*, 73(1):176–186.

CTBTO

1996. Comprehensive Nuclear-Test-Ban Treaty (CTBT). *Treaty Text.*

CTBTO

2010. Operational Manual for Radionuclide Monitoring and the International Exchange of Radionuclide Data. *CTBT/WGB/TL-11,17/18/Rev.5.*

CTBTO

2012. Certification and Surveillance Assessment of Radionuclide Laboratories for Particulate and Noble Gas Sample Analysis. *CTBT/PTS/INF.96/Rev.9.*

CTBTO

2014. Status of signature and ratification. *Available at: The Preparatory Commission for the Comprehensive Nuclear-Test-Ban Treaty Organization. Accessed: 16 December 2014. URL: http://www.ctbto.org/the-treaty/status-of-signature-and-ratification/.*

Currie, L.

1968. Limits for qualitative detection and quantitative determination: application to radiochemistry. *Analytical Chemistry*, 40:586–593.

De Geer, L.-E.

  1996a. Atmospheric Radionuclide Monitoring: a Swedish Perspective. *In: Monitoring a Comprehensive Nuclear Test Ban Treaty*, The Netherlands: Kluwer Academic Publishers:157–177.

De Geer, L.-E.

  1996b. Sniffing out clandestine tests. *Nature*, 382(6591):491–492.

De Geer, L.-E.

  2001. Comprehensive Nuclear-Test-Ban-Treaty: relevant radionuclides. *Kerntechnik*, 66(3):113–120.

De Geer, L.-E.

  2004. Currie detection limits in gamma-ray spectroscopy. *Applied Radiation and Isotopes*, 61(2-3):151–160. Low Level Radionuclide Measurement Techniques - ICRM.

Department of Energy

  2000. United States Nuclear Tests. July 1945 through September 1992. *DOE/NV-209(Rev.15)*.

Divine, R.

  1978. *Blowing on the Wind: The Nuclear Test Ban Debate 1954-1960*. New York: Oxford University Press.

Doll, C., C. Sorensen, T. Bowyer, J. Friese, J. Hayes, E. Hoffmann, and R. Kephart

  2014. Abatement of xenon and iodine emissions from medical isotope production facilities. *Journal of Environmental Radioactivity*, 130:33–43.

Dubasov, Y.

  2010. Underground Nuclear Explosions and Release of Radioactive Noble Gases. *Pure Appl. Geophys. 167, 455-461*.

Dubasov, Y., Popov Y., and Prelovskii V.

  2005. The ARIX-01 Automatic Facility for Measuring Concentrations of Radioactive Xenon Isotopes in the Atmosphere. *Prib. Tekh. Eksp.no. 3, p. 108 [Instrum. Exp. Tech. (engl. Transl.), no. 3, p. 373]*.

Duellmann, C. E., B. Eichler, R. Eichler, H. Gaeggeler, D. Jost, U. Kindler, D. Piguet, S. Soverna, P. Thoerle, N. Trautmann, and A. Tuerler

  2003. Miss Piggy, a californium-252 fission fragment source as a generator of short-lived radionuclides. *Nuclear Instruments and Methods in Physics Research Section A: Accelerators, Spectrometers, Detectors and Associated Equipment*, 512(3):595 − 605.

England, T. and B. Rider

  1994. Evaluation and Compilation of Fission Product Yields. *Los Alamos National Laboratory Report LA-UR-94-3106; ENDF-349*.

Ethan M. Cox and Yuji Arai

2014. Chapter Two - Environmental Chemistry and Toxicology of Iodine. volume 128, Pp. 47 − 96. Academic Press.

Firestone, R.

1999. Table of Isotopes Edition 8. *Wiley Interscience.*

Fontaine, J.-P., F. Pointurier, X. Blanchard, and T. Taffary

2004. Atmospheric xenon radioactive isotope monitoring. *Journal of Environmental Radioactivity,* 72(1-2):129–135.

Furch, T.

2007. *Hochauflösende Beta-Gamma Koinzidenzmessung von Radio-Xenon.* PhD thesis, University of Technology of Vienna.

Galan, M.

2007-2008. Xe-133. *Decay Data Evaluation Project.*

Galan, M.

2007-2012. Xe-133m. *Decay Data Evaluation Project.*

Glasstone, S. and P. Dolan, eds.

1977. *The Effects of Nuclear Weapons, 3rd Edition.* United States Department of Defense and the Energy Research and Development Administration, 653p (Washington, DC: U.S. Government Printing Office).

Gohla, H. and M. Auer

2013. Results of Xenon Laboratory Intercomparison Exercises Performed in 2012. *Science and Technology Conference,* Poster.

Gohla, H., M. Auer, P. Cassette, R. Hague, M. Lechermann, and B. Nadalut

2015. Xenon Concentration Standards used in Laboratory Intercomparisons. *Applied Radiation and Isotopes,* to be published.

Gohla, H., M. Auer, and C. Schlosser

2011. Re-analysis of noble gas ssample from IMS station at laboratories - a review of the results since 2007. *Science and Technology Conference,* Poster.

Gohla, H. and X. Blanchard

2015. Status of laboratory based NG QA/QC program and results of NG inter-comparison exercises. *CTBTO Laboratory Workshop 2015,* Presentation.

Haas, D., S. Biegalski, and K. Foltz Biegalski

2009. Radioxenon production through neutron irradiation of stable xenon gas. *Journal of Radioanalytical and Nuclear Chemistry*, 282(3):677–680.

Haefner, D. and T. Tranter

2007. Methods of Gas Phase Capture of Iodine from Fuel Reprocessing Off-Gas: A Literature Survey. *INL/EXT-07-12299*.

Haynes, W. M., ed.

2014. *Handbook of Chemistry and Physics*, 95th edition edition. Chemical Rubber Company Press.

Kahn, M. and J. Kleinberg

1977. Radiochemistry of iodine. *Nuclear Science Series, National Academy of Sciences - National Research Council*.

Kalinowski, M.

2001. Atmospheric transport modelling related to radionuclide monitoring in support of the Comprehensive Nuclear-Test-Ban Treaty verification. *Kerntechnik*, 66(3):129–133.

Kalinowski, M., A. Axelsson, M. Beanand, X. Blanchard, T. Bowyer, G. Brachet, J. McIntyre, C. Pistner, M. Raith, A. Ringbom, P. Saey, C. Schlosser, T. Stocki, T. Taffary, and R. Ungar

2010. Discrimintation of nuclear explosions against civilian sources based on atmospheric isotopic activity ratios. *Pure and Applied Geophysics*, 167(4-5).

Kepak, F.

1990. Removal of gaseous fission products by adsorption. *Journal of Radioanalytical and Nuclear Chemistry*, 142(1):215–230.

Khariton, Y. and Y. Smirnov

1993. The Khariton version. *Bulletin of the Atomic Scientists*, 5:20–31.

Lessard, E., R. Miltenberger, S. Cohn, S. Musolino, and R. Conard

1984. Protracted exposure to fallout: The rongelap and utirik experience. *Health Physics*, 46(3):511–527.

Medalia, J.

2010. North Koreas 2009 Nuclear Test: Containment, Monitoring, Implications. *Congressional Research Service 7-5700 R41160*.

Mikhailov

1996. USSR Nuclear Weapons Tests and Peaceful Nuclear Explosions. 1949 through 1990. *The Ministry of the Russian Federation for Atomic Energy, the Ministry of Defence of the Russian Federation. RFNC-VNIIEF*.

Nordyke, M.

1998. The Soviet program for peaceful uses of nuclear explosions. *Science & Global Security, Volume 7, pp. 1-117.*

NORM, D.

2011. *Determination of the characteristic limits (decision threshold, detection limit and limits of the confidence interval) for measurements of ionizing radiation - Fundamentals and application (ISO 11929:2010).* Beuth.

NRDC

2006. Natural Resources Defence Council, Press release. *http://www.nrdc.org/media /pressre-leases/061013.asp.*

NRDC

2007. Natural Resources Defence Council: Table of Indian and Pakistani Nuclear Tests 1975-2002. *http://www.nrdc.org/nuclear/nudb/datab22.asp.*

NRDC Archive

2007. Archive of Nuclear Data. *http://www.nrdc.org/nuclear/nudb/datab15.asp.*

Olsen, C. W.

1967. Time history of the cavity pressure and temperature following a nuclear detonation in alluvium. *Journal of Geophysical Research*, 72:5037–5041.

Oughterson, A. and W. Shields, eds.

1956. *Medical effects of the atomic bomb in Japan.* McGraw-Hill Book Company, Inc.

Peräjärvi, K., J. Turunen, J. Hakala, A. Jokinen, I. Moore, H. Penttilä, A. Saastamoinen, T. Siiskonen, H. Toivonen, and J. Äystö

2008. The decay of Xe-133m. *Applied Radiation and Isotopes*, 66(4):530 − 534.

PerkinElmer

2010. Radiometric Reagents Guide 2010-2011. *NEN Radiochemicals.*

Perry, W. and B. Scowcroft

2009. U:S: Nuclear Weapons Policy. *Independent Task Force Report No. 62, Council on Foreign Relations.*

Raith, M.

2006. *Development and quantification of new methods for the determination and preparation of short-lived xenon isotopes for the verification of the Comprehensive Nuclear Test Ban Treaty (CTBT) in a laboratory.* PhD thesis, University of Technology of Vienna.

Ringbom, A., A. Axelsson, M. Aldener, M. Auer, T. Bowyer, T. Fritioff, I. Hoffman, K. Khrustalev, M. Nikkinen, V. Popov, Y. Popov, K. Ungar, and G. Wotawa

2014. Radioxenon detections in the {CTBT} international monitoring system likely related to the announced nuclear test in North Korea on February 12, 2013. *Journal of Environmental Radioactivity*, 128(0):47 − 63.

Ringbom, A., T. Larson, A. Axelsson, K. Elmgren, and C. Johansson

2003. SAUNA−a system for automatic sampling, processing, and analysis of radioactive xenon. *Nuclear Instruments and Methods in Physics Research Section A: Accelerators, Spectrometers, Detectors and Associated Equipment*, 508(3):542−553.

Rodean, H. C.

1968. Understanding and Constructively Using the Effects of Underground Nuclear Explosions. *Reviews of Geophysics and Space Physics*, 6:401−445.

Saey, P.

2009. The influence of radiopharmaceutical isotope production on the global radioxenon background. *Journal of Environmental Radioactivity*, 100(5):396−406.

Saey, P., M. Bean, A. Becker, J. Coyne, R. d'Amours, L.-E. De Geer, R. Hogue, T. Stocki, R. Ungar, and G. Wotawa

2007. A long distance measurement of radioxenon in Yellowknife, Canada, in late October 2006. *Geophysical Research Letters*, 34(20).

Schoengold, C., M. DeMarre, and E. Kirkwood

1996. Radiological Effluents Released from U.S. Continental Tests 1961 through 1992. *DOE/NV-317 (Rev.1) UC-702 United States Department of Energy, Nevada Operations Office, Las Vegas.*

Schroettner, T., I. Schraick, T. Furch, and P. Kindl

2010. A high-resolution, multi-parameter, β-γ coincidence, μ-γ anticoincidence system for radioxenon measurement. *Nuclear Instruments and Methods in Physics Research Section A: Accelerators, Spectrometers, Detectors and Associated Equipment*, 621(1-3):478 − 488.

Schulze, J., M. Auer, and R. Werzi

2000. Low level radioactivity measurement in support of the CTBTO. *Applied Radiation and Isotopes*, 53(1-2):23−30.

Schwaiger, Steger, Schroettner, and Schmitzer

2002. A ultra low level laboratory for nuclear test ban measurements. *Applied Radiation and Isotopes.*

Singh, Rodionov, and Khazov

2008. Xe-135, National Nuclear Data Center, Nuclear Data Sheets 109, 517. *Brookhaven National Laboratory.*

Staudacher, T. and C. Allegre

1982. Terrestrial xenology. *Earth and Planetary Science Letters*, 60(3):389–406.

UNGA

1996. United Nations General Assembly Resolution Number 50/245.

U.S. Congress, Office of Technology Assessment

1989. The Containment of Underground Nuclear Explosions, OTA-ISC-414. *Washington, DC: U.S. Government Printing Office.*

Wiltshire, R.

1985. The preparation and calibration of Californium-252 sources. *Nuclear Instruments and Methods in Physics Research Section A: Accelerators, Spectrometers, Detectors and Associated Equipment*, 236(3):514 − 519.

Windholz, M., S. Budavari, L. Stroumtsos, and M. N. Fertig, eds.

1976. *Merck Index of Chemicals and Drugs (9th ed.)*, number ISBN 0-911910-26-3. J A Majors Company.

Wittner, L.

1997. *The Struggle Against the Bomb : Resisting the Bomb - A History of the World Nuclear Disarmament Movement, 1954-1970,.* Stanford University Press; 1st edition.

Wotawa, G., A. Becker, M. Kalinowski, P. Saey, M. Tuma, and M. Zähringer

2010. Computation and Analysis of the Global Distribution of the Radioxenon Isotope ^{133}Xe based on Emissions from Nuclear Power Plants and Radioisotope Production Facilities and its Relevance for the Verification of the Nuclear-Test-Ban Treaty. *Pure and Applied Geophysics*, 167:541–557.

Wotawa, G., L.-E. De Geer, P. Denier, M. Kalinowski, H. Toivonen, R. D'Amours, F. Desiato, J.-P. Issartel, M. Langer, P. Seibert, A. Frank, C. Sloan, and H. Yamazawa

2003. Atmospheric transport modelling in support of CTBT verification - Overview and basic concepts. *Atmospheric Environment*, 37(18):2529–2537.

Yevgeni A. Karelin, Yan N. Gordeev, Valentin I. Karasev, Vyacheslav M. Radchenko, Yevgeni V. Schimbarev, and Rostislav A. Kuznetsov

1997. Californium-252 neutron sources. *Applied Radiation and Isotopes*, 48:1563 − 1566.

Ziegler, C. and D. Jacobson

1995. *Spying without spies: origins of America's secret nuclear surveillance system.* Praeger, Westport, Conn.

Acknowledgments

I would like to express my sincere gratitude to Ao. Univ. Prof. Dr. Helmuth Böck for sparking my interest in such a lively and interesting field of study and offering me great encouragement and valuable advise. I am deeply indebted to my mentor and friend DI Dr. Thales Schröttner who has helped me in uncountable ways throughout the whole project. His guidance in research and his endless creativity gave me excellent opportunities to learn and develop as a professional.

This work would not have been possible without the financial support of Seibersdorf Laboratories. For the close and fruitful collaboration I want to express my highest appreciation to my colleagues at Seibersdorf, especially the Radiation Safety and Applications group.

I am very grateful to my mother Monika, my sisters Heike and Ines and my brother Ralf for their continuous encouragement throughout the years. Finally, I wish to thank Melissa for her never-ending patience and support.